

Exact Potts/Tutte Polynomials for Hammock Chain Graphs

Yue Chen and Robert Shrock

C. N. Yang Institute for Theoretical Physics and

Department of Physics and Astronomy

Stony Brook University, Stony Brook, NY 11794

We present exact calculations of the q -state Potts model partition functions and the equivalent Tutte polynomials for chain graphs comprised of m repeated hammock subgraphs H_{e_1, \dots, e_r} connected with line graphs of length e_g edges, such that the chains have open or cyclic boundary conditions (BC). Here, H_{e_1, \dots, e_r} is a hammock (series-parallel) subgraph with r separate paths along “ropes” with respective lengths e_1, \dots, e_r edges, connecting the two end vertices. We denote the resultant chain graph as $G_{\{e_1, \dots, e_r\}, e_g, m; BC}$. We discuss special cases, including chromatic, flow, and reliability polynomials. In the case of cyclic boundary conditions, the zeros of the Potts partition function in the complex q function accumulate, in the limit $m \rightarrow \infty$, onto curves forming a locus \mathcal{B} , and we study this locus.

I. INTRODUCTION

The q -state Potts model has long been of interest in the study of phase transitions and critical phenomena [1, 2]. On a lattice, or, more generally, on a graph G , at temperature T , the partition function for the Potts model is

$$Z = \sum_{\{\sigma_i\}} e^{-\beta\mathcal{H}} , \quad (1.1)$$

where $\beta = 1/(k_B T)$, k_B is the Boltzmann constant, and the Hamiltonian is

$$\mathcal{H} = -J \sum_{e_{ij}} \delta_{\sigma_i \sigma_j} , \quad (1.2)$$

where J is the spin-spin interaction constant, i and j denote vertices (= sites) in G , e_{ij} is the edge (= bond) connecting them, and σ_i are classical spins taking on values in the set $\{1, \dots, q\}$. We use the notation

$$K = \beta J , \quad y = e^K , \quad v = y - 1 . \quad (1.3)$$

We denote the partition function of the Potts model on a graph G as $Z(G, q, v)$. Thus, for the Potts ferromagnet (FM, $J > 0$) and antiferromagnet (AFM, $J < 0$), the physical ranges of v are $v \geq 0$ and $-1 \leq v \leq 0$, respectively. On a graph G , we denote the Potts partition function as $Z(G, q, v)$. For the Potts antiferromagnet (PAF), $J < 0$ so that, as $T \rightarrow 0$, $K \rightarrow -\infty$, i.e., $v \rightarrow -1$; hence, in this limit, the only contributions to the PAF partition function are from spin configurations in which adjacent spins have different values. The resultant $T = 0$ PAF partition function is therefore precisely the chromatic polynomial $P(G, q)$ of the graph G , which counts the number of ways of assigning q colors to the vertices of G , subject to the condition that no two adjacent vertices have the same color [3]-[7]. That is,

$$Z(G, q, -1) = P(G, q) . \quad (1.4)$$

This is called a proper q -coloring of (the vertices of) G . The zeros of $P(G, q)$ in the complex q plane are called chromatic zeros of G . An important feature of the antiferromagnetic Potts model is that for sufficiently large q on a given graph G with finite maximal vertex degree, it has a nonzero entropy per site at zero temperature, $S_0 = k_B \ln W$, where W denotes the ground state degeneracy per site [2, 8–10]. This is important as an exception to the third law of thermodynamics, that the entropy per site vanishes at zero temperature. A physical example of this phenomenon is the residual entropy of ice [11]-[13]. The Potts partition function $Z(G, q, v)$ is equivalent to a function of fundamental importance in mathematical

graph theory, the Tutte polynomial, $T(G, x, y)$ [14]-[18] (see Eq. (2.21) below). We will therefore often refer to these together as the Potts/Tutte polynomial.

In Ref. [19] with S.-H. Tsai, an exact expression was given (in Eq. (3.7) of [19]) for the partition function of the zero-temperature Potts antiferromagnet, or equivalently, the chromatic polynomial, of a “hammock” graph, denoted $H_{k,r}$, defined as a series-parallel graph containing two end vertices with r separate “ropes” (paths) joining these two end-vertices, such that on each rope there are k “knots” (vertices), including the end vertices, i.e., $k - 1$ edges on each rope. This was part of a program of studies [19]-[22] of families of graphs having the property that in the limit $r \rightarrow \infty$ for fixed k (denoted L_r below), the magnitudes of the chromatic zeros are unbounded, and the continuous accumulation set of chromatic zeros extends to the origin of the $1/q$ plane. Here we will generalize this family of graphs to encompass the case where there are different numbers of edges e_j , $j = 1, \dots, r$, on the different ropes and hence denote this hammock graph as H_{e_1, \dots, e_r} . In Ref. [23] with S.-H. Tsai, exact results were given for the chromatic polynomial of open and cyclic chain graphs composed of m repetitions of p -sided polygons connected to each other by line segments of length e_g edges. Each polygon can be described as a hammock graph with $r = 2$ ropes, viz., H_{e_1, e_2} (where e_1 and e_2 are, in general, different), such that the right-hand end-vertex of a given H_{e_1, e_2} subgraph is connected to a line graph consisting of e_g edges, which then connects to the left-hand end-vertex of the next H_{e_1, e_2} subgraph in the chain. In [24], one of us generalized [23] to a calculation of the full Potts/Tutte polynomial for these graphs. A motivation for the work in [24] was to elucidate how the results for the zero-temperature Potts antiferromagnet obtained in [23] generalize to finite-temperature and also to ferromagnetic as well as antiferromagnetic spin-spin couplings.

In this paper we present a calculation of the Potts/Tutte polynomial for a further generalization of these families of graphs, namely for a chain graph comprised of m hammock subgraphs H_{e_1, \dots, e_r} such that the right-hand end vertex of a given hammock subgraph is connected to a line graph of length e_g edges, which then connects to the left-hand end-vertex of the next hammock subgraph. We consider both open (free) and cyclic longitudinal boundary conditions (BC) for the chain, and thus denote a general chain graph of this type as $G_{\{e_1, \dots, e_r\}, e_g, m; BC}$. We will use a compact notation to denote the set of edges in each hammock subgraph as

$$\{e\}_r \equiv \{e_1, e_2, \dots, e_r\} , \quad (1.5)$$

so that a hammock subgraph is denoted $H_{\{e\}_r}$, and the full chain graph comprised of m hammock subgraphs $H_{\{e\}_r}$ connected with line graphs of length e_g edges, with longitudinal

boundary conditions denoted as $BC = o$ for open or $BC = c$ for cyclic, is denoted

$$G_{\{e\}_r, e_g, m; BC} \equiv G_{\{e_1, \dots, e_r\}, e_g, m; BC} , \quad BC = o \text{ or } c . \quad (1.6)$$

In Fig. 1 we show illustrative examples of the open and cyclic $r = 3$ hammock chain graphs with $(\{e_1, e_2, e_3\}, e_g, m) = (\{2, 3, 4\}, 2, 3)$, i.e., $G_{\{2,3,4\}, 2, 3; o}$ and $G_{\{2,3,4\}, 2, 3; c}$. These hammock chain graphs are recursive in the sense of [25, 26]; i.e., $G_{\{e\}_r, e_g, m+1; o}$ can be obtained by attaching another $H_{\{e\}_r}$ subgraph and associated line graph of length e_g edges to $G_{\{e\}_r, e_g, m; o}$, and similarly, $G_{\{e\}_r, e_g, m+1; c}$ can be obtained by cutting a $G_{\{e\}_r, e_g, m; c}$ graph at any of the $H_{\{e\}_r}$ end-vertices and inserting and gluing a $H_{\{e\}_r}$ subgraph with its associated line graph of length e_g edges. It is clear that the graph $G_{\{e\}_r, e_g, m; BC}$ with $BC = o$ or $BC = c$ is unchanged if one permutes the values of the individual edges e_j in the set $\{e\}_r$. Hence, without loss of generality, by convention, when considering specific sets $\{e\}_r$, we take $e_1 \leq e_2 \leq \dots \leq e_r$. Obviously, these are planar graphs.

If $r = 1$, then $G_{e_1, e_g, m; o}$ and $G_{e_1, e_g, m; c}$ reduce simply to the line graph with $n = m(e_1 + e_g) + 1$ vertices and the circuit graph with $n = m(e_1 + e_g)$ vertices, respectively. Since the Potts/Tutte polynomials for these are well-known, we will focus on the cases with $r \geq 2$ here. If $r = 2$, then each hammock subgraph is a polygon with p sides, where

$$r = 2 : \quad p = e_1 + e_2 . \quad (1.7)$$

This was the case studied in Refs. [23, 24]. Illustrative figures of the polygon chain graphs were given in Fig. 1 of [23]. As noted, the chromatic polynomial for the case of arbitrary r with $e_i = e_j$ for all $i, j \in \{1, \dots, r\}$ was studied in [19]. In addition to being of interest in its own right, the generalization considered here is valuable because it shows how the previous $r = 2$ results in [23, 24] arise as special cases of general- r properties and how the results in [19] arise as $v = -1$ special cases of general physical values of v , namely $-1 \leq v < \infty$.

Many results are simplest when expressed in terms of Tutte polynomials, so we will give these first, and then discuss the corresponding Potts model partition functions. In general, for a given graph G , although the Tutte polynomial $T(G, x, y)$ is equivalent to the Potts model partition function $Z(G, q, v)$, it is valuable to include results expressed in terms of the latter as well as the former, because the variable q plays an important physical role in the Hamiltonian formulation of Eqs. (1.1) and (1.2), and only in the Potts partition function does this variable appear by itself; in $T(G, x, y)$ it only appears in combination with the temperature-dependent variable $y = v + 1$, as $x = 1 + q/v$. After giving these results, we then present special cases of one-variable polynomials, including the chromatic, flow, and reliability polynomials.

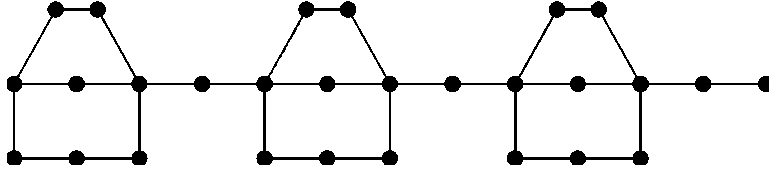


FIG. 1: Illustrations of hammock chain graphs with $r = 3$, $G_{\{e\}_{r=3, e_g, m; o}}$ and $G_{\{e\}_{r=3, e_g, m; c}}$, where $\{e\}_{r=3} \equiv \{e_1, e_2, e_3\} = \{2, 3, 4\}$, $e_g = 2$, and $m = 3$. For the cyclic hammock chain graph, the vertex on the right end is identified with the vertex on the left end of the chain, while for the open hammock chain graph, it is a distinct vertex.

We mention some previous related work by other authors. Read and Tutte calculated the chromatic polynomial for the case $r = 3$, namely $P(H_{\{e\}_{r=3}}, q)$, in [5]. In Ref. [27], Sokal calculated the Potts model partition function $Z(H_{\{e\}_r}, q, v)$, for general r and generalized this further to a multivariate case where the v parameters are different for different edges (see also [28]). To our knowledge, the Tutte polynomial and corresponding Potts model partition function have not previously been calculated for the cases considered here, namely an open or cyclic chain graph for general r and m , $G_{\{e\}_r, e_g, m; BC}$. We will apply our results to study partition function zeros and their accumulation locus in the limit $m \rightarrow \infty$. As will be shown, for fixed r , $\{e\}_r$, and e_g , in the limit $m \rightarrow \infty$, the zeros of $Z(G_{\{e\}_r, e_g, m; o}, q, v)$ are discrete, with no nontrivial continuous accumulation locus. In contrast, as was already clear from the results in [23, 24], for fixed r , $\{e\}_r$, and e_g , in the same limit $m \rightarrow \infty$, the zeros of the chromatic polynomial and Potts/Tutte polynomial for the cyclic hammock chain graph accumulate on a nontrivial continuous locus. Hence, in this paper we will focus mainly on the cyclic chain graphs.

II. SOME BACKGROUND

In this section we give some relevant background on graph theory and the Potts and Tutte polynomials (see, e.g., [17, 18, 26]). In general, a graph $G = (V, E)$ is defined by its set of vertices (sites), V , and its set of edges (bonds), E . We denote the number of vertices in G as $n = n(G) = |V|$ and the number of edges in G as $e(G) = |E|$. The degree Δ of a vertex $v_i \in V$ is defined as the number of edges that connect to this vertex. The number of connected components of a graph is denoted $k(G)$. The number of linearly independent

circuits in a graph G , called the cyclomatic number of G , is denoted $c(G)$ and satisfies the relation $c(G) = e(G) + k(G) - n(G)$. A spanning subgraph of G , denoted $G' = (V, E')$, is a subgraph of $G = (V, E)$ that has the same vertex set V as G and an edge set $E' \subseteq E$.

For the open and cyclic hammock chain graphs, the number of vertices and edges are

$$n(G_{\{e\}_r, e_g, m; o}) = m \left[\left(\sum_{j=1}^r e_j \right) + e_g - (r - 1) \right] + 1, \quad (2.1)$$

$$n(G_{\{e\}_r, e_g, m; c}) = m \left[\left(\sum_{j=1}^r e_j \right) + e_g - (r - 1) \right], \quad (2.2)$$

and

$$e(G_{\{e\}_r, e_g, m; o}) = e(G_{\{e\}_r, e_g, m; c}) = m \left[\left(\sum_{j=1}^r e_j \right) + e_g \right]. \quad (2.3)$$

The number of linearly independent circuits on the hammock chain graphs are thus

$$c(G_{\{e\}_r, e_g, m; o}) = m(r - 1) \quad (2.4)$$

and

$$c(G_{\{e\}_r, e_g, m; c}) = m(r - 1) + 1. \quad (2.5)$$

As is evident from Eqs. (2.1) and (2.2), there are several different ways to take the limit of infinitely many vertices. These include the limits

1. L_{e_g} : $e_g \rightarrow \infty$ with r , $\{e\}_r$, and m fixed;
2. L_{e_j} : $e_j \rightarrow \infty$ with other $e_\ell \in \{e\}_r$, $\ell \neq j$ fixed, and r , e_g , and m fixed;
3. L_r : $r \rightarrow \infty$ with each e_j in the expanding set $\{e\}_r$ finite and e_g and m fixed;
4. L_m : $m \rightarrow \infty$ with r , $\{e\}_r$ and e_g fixed.

In the limits L_{e_g} , L_{e_j} , and L_m on $G_{\{e\}_r, e_g, m; BC}$, all vertices have bounded degree, whereas in the limit L_r , the end-vertices of each hammock subgraph in the chain have infinite degree.

In the context of chromatic polynomials, in [19], Tsai and Shrock applied their calculations of $P(H_{k,r}, q)$ to the L_r limit, while in [23] for $r = 2$, these authors considered several limits with detailed results for the L_m limit. For general physical v , Ref. [24] studied the L_m limit, and here also we will apply our new calculations in particular to this L_m limit, i.e., the limit of an infinitely long hammock chain graph. We will thus introduce the following compact

notation. We denote the limit as $m \rightarrow \infty$ of $G_{\{e\}_r, e_g, m; BC}$ with a given set of values of r , $\{e\}_r$, and e_g as

$$\lim_{m \rightarrow \infty} G_{\{e\}_r, e_g, m; BC} \equiv \{G_{\{e\}_r, e_g; BC}\}. \quad (2.6)$$

We consider cases with both zero and nonzero e_g . Formally, one could allow one or more of the edges $e_j \in \{e\}_r$ in the hammock subgraphs to be zero. However, insofar as one is interested in the application to the Potts spin model, one would take the minimum value $\min(e_j) \geq 1$ for $e_j \in \{e\}_r$ to maintain the physical property that spins do not interact with themselves. Note that if $e_1 = 0$ and any other $e_j \in \{e\}_r$ is equal to 1, then the graph $G_{\{e\}_r, e_g, m; BC}$ contains loop(s), so in the physical context, a spin would interact with itself. We therefore assume $e_j \geq 1$ for all $e_j \in \{e\}_r$ here. The presence of a loop in a graph G also causes the chromatic polynomial of this graph to vanish identically, since this loop renders it impossible to satisfy the proper q -coloring condition.

A Δ -regular graph G is defined as a graph with the property that all of its vertices have the same degree, Δ . In a Δ -regular graph, one has the relation $\Delta = 2e(G)/n(G)$. A hammock chain graph is not, in general, a Δ -regular graph. However, in the limit of an infinitely long hammock chain, we may define an effective vertex degree as

$$\Delta_{\text{eff}}(\{G_{\{e\}_r, e_g}\}) = \lim_{m \rightarrow \infty} \frac{2e(G_{\{e\}_r, e_g, m; BC})}{n(G_{\{e\}_r, e_g, m; BC})}, \quad (2.7)$$

where we omit the subscript BC in $\Delta_{\text{eff}}(\{G_{\{e\}_r, e_g}\})$ because this is independent of the boundary condition. Note that with cyclic boundary conditions, the ratio $2e(G_{\{e\}_r, e_g, m; c})/n(G_{\{e\}_r, e_g, m; c})$ is independent of m . We calculate

$$\Delta_{\text{eff}}(\{G_{\{e\}_r, e_g}\}) = \frac{2[(\sum_{j=1}^r e_j) + e_g]}{(\sum_{j=1}^r e_j) + e_g - (r - 1)}. \quad (2.8)$$

In this $m \rightarrow \infty$ limit, a fraction f_2 of the vertices, namely the ones in the interior of the ropes on each hammock subgraph and in interior of the line segments between each hammock subgraph, have degree 2, while a fraction f_{he} of the vertices, which are hammock endpoint (he) vertices, have degree $r + 1$. These fractions are

$$f_2 = \frac{(\sum_{j=1}^r e_j) + e_g - (r + 1)}{(\sum_{j=1}^r e_j) + e_g - (r - 1)} = 1 - \frac{2}{(\sum_{j=1}^r e_j) + e_g - (r - 1)} \quad (2.9)$$

and

$$f_{he} = \frac{2}{(\sum_{j=1}^r e_j) + e_g - (r - 1)} = 1 - f_2. \quad (2.10)$$

Thus,

$$\Delta_{\text{eff}}(\{G_{\{e\}_r, e_g}\}) = 2f_2 + (r + 1)f_{he}. \quad (2.11)$$

For example, in the $m \rightarrow \infty$ limit of the open and cyclic hammock chain graphs with $r = 3$, $\{e_1, e_2, e_3\} = \{2, 3, 4\}$ and $e_g = 2$ in Fig. 1, we have $f_2 = 7/9$, $f_{he} = 2/9$ and $\Delta_{\text{eff}} = 22/9 = 2.44444\dots$. We note the limits

$$\lim_{(\sum_{j=1}^r e_j) \rightarrow \infty} \Delta_{\text{eff}}(\{G_{\{e\}_r, e_g}\}) = 2 \quad \text{for fixed } e_g, r \quad (2.12)$$

and

$$\lim_{e_g \rightarrow \infty} \Delta_{\text{eff}}(\{G_{\{e\}_r, e_g}\}) = 2 \quad \text{for fixed } \{e\}_r, r. \quad (2.13)$$

As is evident in Eq. (2.8), the value of $\Delta_{\text{eff}}(\{G_{\{e\}_r, e_g}\})$ is determined by an interplay of the degree-2 vertices in the interiors of the r ropes and in the line segments between the hammock subgraphs, on the one hand, and the degree- $(r+1)$ vertices at the ends of each hammock subgraph. This is illustrated, for example, by a family of (open or cyclic) hammock chain graphs in which all of the edges $e_j \in \{e\}_r$ have the common value e_{com} . For the $m \rightarrow \infty$ limit of a hammock graph in this family (with either boundary condition),

$$e_j = e_{\text{com}} \Rightarrow \Delta_{\text{eff}}(\{G_{\{e\}_r, e_g}\}) = \frac{2(re_{\text{com}} + e_g)}{r(e_{\text{com}} - 1) + e_g + 1}. \quad (2.14)$$

Now consider the limit $r \rightarrow \infty$ with fixed finite e_g ; if $e_{\text{com}} = 1$, then

$$e_{\text{com}} = 1 \Rightarrow \lim_{r \rightarrow \infty} \Delta_{\text{eff}}(\{G_{\{e\}_r, e_g}\}) = \infty, \quad (2.15)$$

whereas if $e_{\text{com}} \geq 2$, then the effective vertex degree remains finite in this limit:

$$e_{\text{com}} \geq 2 \Rightarrow \lim_{r \rightarrow \infty} \Delta_{\text{eff}}\{G_{\{e\}_r, e_g}\} = \frac{2e_{\text{com}}}{e_{\text{com}} - 1}. \quad (2.16)$$

The Tutte polynomial of a graph G [14]-[18], which we denote as $T(G, x, y)$, is

$$T(G, x, y) = \sum_{G' \subseteq G} (x-1)^{k(G')-k(G)} (y-1)^{c(G')}. \quad (2.17)$$

where G' is a spanning subgraph of G . Since $k(G') - k(G) \geq 0$ and $c(G') \geq 0$, this is, indeed, a polynomial in the given variables x and y . (The first factor can equivalently be written as $(x-1)^{r(G)-r(G')}$, where $r(G) = n(G) - k(G)$ is the rank of G , since $r(G) - r(G') = k(G') - k(G)$, owing to the property that $n(G') = n(G)$.) Although the starting point for the definition of the Potts model partition function is the Hamiltonian form $Z = \sum_{\sigma_i} \exp[K \sum_{e_{ij}} \delta_{\sigma_i, \sigma_j}]$, it can be written as a similar sum over contributions from spanning subgraphs without explicit reference to the sum over spin configurations, namely as [29]

$$Z(G, q, v) = \sum_{G' \subseteq G} q^{k(G')} v^{e(G')}. \quad (2.18)$$

Since $k(G') \geq 1$ and $e(G') \geq 0$, this shows that $Z(G, q, v)$ is a polynomial in q and v . Given that $k(G') \geq 1$, $Z(G, q, v)$ always contains an overall factor of q , so one can define a reduced partition function $Z_r(G, q, v)$ as

$$Z_r(G, q, v) = q^{-1}Z(G, q, v) . \quad (2.19)$$

An elementary property of $Z(G, q, v)$ for an arbitrary graph G is that if $v = 0$, then the only nonzero contribution to the sum in Eq. (2.18) is from the spanning subgraph with no edges, \mathcal{E}_n , which has $k(G') = n(G)$ components, so

$$v = 0 \Rightarrow Z(G, q, v) = q^{n(G)} . \quad (2.20)$$

From (2.17) and (2.18), it follows that $Z(G, q, v)$ and $T(G, x, y)$ are simply related, according to

$$\begin{aligned} Z(G, q, v) &= (x - 1)^{k(G)}(y - 1)^{n(G)}T(G, x, y) \\ &= (q/v)^{k(G)}v^{n(G)}T(G, x, y) , \end{aligned} \quad (2.21)$$

where

$$x = 1 + \frac{q}{v} , \quad y = v + 1 . \quad (2.22)$$

Note that

$$q = (x - 1)(y - 1) . \quad (2.23)$$

Given a graph G , let us denote $G - e$ as the graph obtained by deleting the edge $e \in E$ and G/e as the graph obtained by deleting the edge e and identifying the two vertices that were connected by this edge of G (known as a contraction of G on e .) An edge that connects a vertex back to itself is called a loop. An edge which, if cut, increases the number of disjoint components in G , is called a bridge. A graph consisting of n vertices with no edges is denoted \mathcal{E}_n , the “empty” graph. The Tutte polynomial satisfies the properties $T(\mathcal{E}_n, x, y) = 1$, $T(G, x, y) = xT(G - e, x, y)$ if e is a bridge, and $T(G, x, y) = yT(G/e, x, y)$ if e is a loop. If e is neither a bridge nor a loop, then $T(G, x, y)$ satisfies the deletion-contraction relation (DCR)

$$T(G, x, y) = T(G - e, x, y) + T(G/e, x, y) . \quad (2.24)$$

As mentioned, the special case $v = -1$ corresponds to the $T = 0$ Potts antiferromagnet, and is equivalent to setting $x = 1 - q$ and $y = 0$. Thus, given that the chromatic polynomial $P(G, q) = Z(G, q, v = -1)$, one has

$$Z(G, q, -1) = P(G, q) = (-q)^{k(G)}(-1)^{n(G)}T(G, 1 - q, 0) . \quad (2.25)$$

Recall that for the circuit graph with n vertices, C_n ,

$$T(C_n, x, y) = \frac{x^n - x}{x - 1} + y \quad (2.26)$$

and equivalently

$$Z(C_n, q, v) = (q + v)^n + (q - 1)v^n . \quad (2.27)$$

Note that $T(C_1, x, y) = y$ and, if $n \geq 2$, then $T(C_n, x, y)$ can alternately be expressed as $T(C_n, x, y) = (\sum_{j=1}^{n-1} x^j) + y$. To save space, we will sometimes use the compact notation

$$c \equiv q - 1 = xy - x - y . \quad (2.28)$$

(The reader should not confuse this q -dependent quantity c with the G -dependent cyclotomic number, $c(G$.) It is also useful to define a polynomial of degree $n - 2$ in q denoted D_n that appears in various expressions for Tutte and Potts model polynomials [30]. Extracting the factor $q(q - 1)$ in $P(C_n, q)$, one can write

$$P(C_n, q) = (q - 1)^n + (q - 1)(-1)^n = q(q - 1)D_n , \quad (2.29)$$

where, for $n \geq 2$,

$$D_n = \sum_{j=0}^{n-2} (-1)^j \binom{n-1}{j} q^{n-2-j} = (q - 1)^{n-2} \sum_{j=0}^{n-2} (1 - q)^{-j} , \quad (2.30)$$

and $\binom{r}{s} = r!/[s!(r - s)!]$ is the binomial coefficient. For $n = 1$, $P(C_1, q) = 0$ and hence also $D_1 = 0$. Some expressions for D_n with higher n include $D_2 = 1$, $D_3 = q - 2$, $D_4 = q^2 - 3q + 3$, $D_5 = (q - 2)(q^2 - 2q + 2)$, etc. Since $P(C_n, q)$ is of degree n in q , it follows from the definition (2.29) that for $n \geq 2$, D_n is of degree $n - 2$ in q . Some identities obeyed by D_n are listed in the Appendix; see also [30].

III. CALCULATIONS AND RESULTS

Using an iterative application of the deletion-contraction theorem, we have calculated the Tutte polynomial and equivalent Potts model partition function for the open and cyclic hammock chain graphs with general r , $\{e\}_r$, e_g , and m , $G_{\{e\}_r, e_g, m; o}$ and $G_{\{e\}_r, e_g, m; c}$. For the open hammock chain graph $G_{\{e\}_r, e_g, m; o}$, we obtain

$$T(G_{\{e\}_r, e_g, m; o}, x, y) = (\lambda_{T,0})^m , \quad (3.1)$$

where

$$\lambda_{T,0} = \frac{x^{e_g}}{q(x-1)^{r-1}} \left[\prod_{j=1}^r (x^{e_j} + c) + c \prod_{j=1}^r (x^{e_j} - 1) \right]. \quad (3.2)$$

For the cyclic hammock chain graph $G_{\{e\}_r, e_g, m; c}$ we calculate

$$T(G_{\{e\}_r, e_g, m; c}, x, y) = \frac{1}{x-1} \left[(\lambda_{T,0})^m + c(\lambda_{T,1})^m \right], \quad (3.3)$$

where c and $\lambda_{T,0}$ were given in Eqs. (2.28) and (3.2), and

$$\lambda_{T,1} = \frac{1}{q(x-1)^{r-1}} \left[\prod_{j=1}^r (x^{e_j} + c) - \prod_{j=1}^r (x^{e_j} - 1) \right]. \quad (3.4)$$

These expressions for $\lambda_{T,0}$ and $\lambda_{T,1}$, and for $T(G_{\{e\}_r, e_g, m; o}, x, y)$ and $T(G_{\{e\}_r, e_g, m; c}, x, y)$, are invariant under a permutation of the r edges in the set $\{e\}_r = \{e_1, e_2, \dots, e_r\}$. This is a consequence of the fact that the graphs $G_{\{e\}_r, e_g, m; o}$ and $G_{\{e\}_r, e_g, m; c}$ themselves are invariant under such a permutation.

Since $T(G, x, y)$ is a polynomial in x and y for any graph G , it follows that the expressions in square brackets for $\lambda_{T,0}$ and $\lambda_{T,1}$ each contain a factor of $q(x-1)^{r-1}$ which cancels the prefactor $1/[q(x-1)^{r-1}]$. The overall prefactor $1/(x-1)$ in Eq. (3.3) is also cancelled. Since $x = 1 \Rightarrow c = -1$, the numerator of $T(G_{\{e\}_r, e_g, m; c}, x, y)$ has the limit $(\lambda_{T,0})^m - (\lambda_{T,1})^m$ as $x \rightarrow 1$, and hence this cancellation of the prefactor $1/(x-1)$ in Eq. (3.3) implies that, for arbitrary $\{e\}_r$ and e_g ,

$$\lambda_{T,0;x=1} = \lambda_{T,1;x=1}, \quad (3.5)$$

where the evaluation at $x = 1$ is indicated in a subscript. We give the general expression for $\lambda_{T,0;x=1}$ below in Eq. (3.15).

One can express $\lambda_{T,0}$ and $\lambda_{T,1}$ equivalently in a form in which the r -fold products in Eqs. (3.2) and (3.4) are multiplied out. For this purpose, we introduce some compact notation. Certain terms involve x raised to the power

$$\sum_{j=1}^r e_j \equiv (\sum e_j)_r, \quad (3.6)$$

where the second term will be taken as shorthand notation for the first. Other terms involve sums, each term of which is x raised to a power consisting of the sum $\sum_{j=1}^r e_j$ with d edges deleted, which will be denoted as $(\sum e_j)_{r-d}$. There are $\binom{r}{d}$ ways to choose the subset of d edges in $\{e\}_r$ to be deleted, and hence these sums will consist of $\binom{r}{d}$ terms. Expressions for the corresponding Potts model partition functions involve factors of the form $v^{(\sum e_j)_d} (q + v)^{(\sum e_j')_{r-d}}$, where here the notation for the exponent of v in the factor $v^{(\sum e_j)_d}$ means a sum

of the d edges in $\{e\}_r$ that are deleted in the other factor, $(q+v)^{(\sum e_j)r-d}$. We also recall the Heaviside step function, $\theta(x)$, defined as $\theta(x) = 1$ if $x \geq 0$ and $\theta(x) = 0$ if $x < 0$. For the hammock chain graphs $G_{\{e\}_r, e_g, m; BC}$, multiplying out the r -fold products in Eqs. (3.2) and (3.4), we obtain the following equivalent expressions:

$$\begin{aligned} \lambda_{T,0} = & \frac{\theta(r-2)x^{e_g}}{(x-1)^{r-1}} \left[x^{(\sum e_j)r} + \theta(r-3)cD_2 \sum_{\binom{r}{2} \text{ terms}} x^{(\sum e_j)r-2} \right. \\ & \left. + \theta(r-4)cD_3 \sum_{\binom{r}{3} \text{ terms}} x^{(\sum e_j)r-3} + \dots + cD_r \right] \end{aligned} \quad (3.7)$$

and

$$\begin{aligned} \lambda_{T,1} = & \frac{1}{(x-1)^{r-1}} \left[\theta(r-2)D_2 \sum_{r \text{ terms}} x^{(\sum e_j)r-1} + \theta(r-3)D_3 \sum_{\binom{r}{2} \text{ terms}} x^{(\sum e_j)r-2} \right. \\ & \left. + \theta(r-4)D_4 \sum_{\binom{r}{3} \text{ terms}} x^{(\sum e_j)r-3} + \dots + D_{r+1} \right], \end{aligned} \quad (3.8)$$

In Eqs. (3.7) and (3.8) (and Eqs. (4.7) and (4.8) below), we include D_2 factors to show the general structure, but note that $D_2 = 1$. These forms for $\lambda_{T,0}$ and $\lambda_{T,1}$ are useful partly because there are cancellations that occur among certain terms in the expressions (3.2) and (3.4) involving r -fold products.

For $r = 2$, these general results reduce to

$$\lambda_{T,0;r=2} = \frac{x^{e_g}}{x-1} \left[x^{e_1+e_2} + c \right] \quad (3.9)$$

and

$$\lambda_{T,1;r=2} = \frac{1}{x-1} \left[(x^{e_1} + x^{e_2}) + D_3 \right], \quad (3.10)$$

in agreement with Eqs. (3.2) and (3.4) in [24]. For $r = 3$, our general results yield the explicit expressions

$$\lambda_{T,0;r=3} = \frac{x^{e_g}}{(x-1)^2} \left[x^{e_1+e_2+e_3} + c(x^{e_1} + x^{e_2} + x^{e_3}) + cD_3 \right] \quad (3.11)$$

and

$$\lambda_{T,1;r=3} = \frac{1}{(x-1)^2} \left[(x^{e_1+e_2} + x^{e_1+e_3} + x^{e_2+e_3}) + D_3(x^{e_1} + x^{e_2} + x^{e_3}) + D_4 \right], \quad (3.12)$$

while for $r = 4$ they yield

$$\begin{aligned}\lambda_{T,0;r=4} &= \frac{x^{e_g}}{(x-1)^3} \left[x^{e_1+e_2+e_3+e_4} \right. \\ &\quad + c(x^{e_1+e_2} + x^{e_1+e_3} + x^{e_1+e_4} + x^{e_2+e_3} + x^{e_2+e_4} + x^{e_3+e_4}) \\ &\quad \left. + cD_3(x^{e_1} + x^{e_2} + x^{e_3} + x^{e_4}) + cD_4 \right] \end{aligned} \quad (3.13)$$

and

$$\begin{aligned}\lambda_{T,1;r=4} &= \frac{1}{(x-1)^3} \left[(x^{e_1+e_2+e_3} + x^{e_1+e_2+e_4} + x^{e_1+e_3+e_4} + x^{e_2+e_3+e_4}) \right. \\ &\quad + D_3(x^{e_1+e_2} + x^{e_1+e_3} + x^{e_1+e_4} + x^{e_2+e_3} + x^{e_2+e_4} + x^{e_3+e_4}) \\ &\quad \left. + D_4(x^{e_1} + x^{e_2} + x^{e_3} + x^{e_4}) + D_5 \right]. \end{aligned} \quad (3.14)$$

In a similar manner, one can evaluate our general formulas (3.2) and (3.4), or equivalently, (3.7) and (3.8), to obtain explicit expressions for $\lambda_{T,0}$ and $\lambda_{T,1}$ for higher values of r .

For several applications, including calculations of reliability polynomials and various graphical quantities such as the number of spanning trees and the number of connected spanning subgraphs of $G_{\{e\}_r, e_g, m; 0}$ and $G_{\{e\}_r, e_g, m; c}$, one needs to evaluate $T(G_{\{e\}_r, e_g, m; BC}, x, y)$ at $x = 1$. Since Eqs. (3.2) and (3.4) have factors $1/(x-1)^{r-1}$, which are singular at $x = 1$, we use an $(r-1)$ -fold application of L'Hôpital's rule for the evaluations of $\lambda_{T,0}$ and $\lambda_{T,1}$ at $x = 1$, together with an additional use of L'Hôpital's rule to deal with the $1/(x-1)$ factor in $T(G_{\{e\}_r, e_g, m; c}, x, y)$. For clarity, we sometimes append the value of r and x in subscripts on $\lambda_{T,0}$ and $\lambda_{T,1}$. We find

$$\lambda_{T,0;x=1} = \lambda_{T,1;x=1} = \frac{1}{(y-1)} \left[\prod_{j=1}^r (e_j + y - 1) - \prod_{j=1}^r e_j \right]. \quad (3.15)$$

As is evident from Eq. (3.15), the second term is always cancelled by a term $\prod_{j=1}^r e_j$ arising from the first product in the square brackets. As examples of the general formula (3.15), if $r = 2$, then

$$\lambda_{T,0;x=1,r=2} = \lambda_{T,1;x=1,r=2} = e_1 + e_2 + y - 1, \quad (3.16)$$

and if $r = 3$,

$$\lambda_{T,0;x=1,r=3} = \lambda_{T,1;x=1,r=3} = (e_1 e_2 + e_1 e_3 + e_2 e_3)$$

$$+ (y - 1)(e_1 + e_2 + e_3) + (y - 1)^2 . \quad (3.17)$$

Hence, for the open hammock chain graph,

$$T(G_{\{e\}_{r,e_g,m;o}, 1, y) = (\lambda_{T,0;x=1})^m . \quad (3.18)$$

For the cyclic hammock chain, given the equality (3.5), calculating the derivatives $\partial\lambda_{T,0}/\partial x$, and $\partial\lambda_{T,1}/\partial x$ and evaluating them at $x = 1$, we have

$$\begin{aligned} T(G_{\{e\}_{r,e_g,m;c}, 1, y) &= (\lambda_{T,0})^{m-1} \left[m \left(\frac{\partial\lambda_{T,0}}{\partial x} - \frac{\partial\lambda_{T,1}}{\partial x} \right) + (y - 1)\lambda_{T,0} \right] \Big|_{x=1} \\ &= (\lambda_{T,0;x=1})^{m-1} \left[(me_g + y - 1)\lambda_{T,0;x=1} + m \prod_{j=1}^r e_j \right] , \end{aligned} \quad (3.19)$$

where in Eqs. (3.18) and (3.19), $\lambda_{T,0;x=1}$ is given by Eq. (3.15). For example, for $r = 2$,

$$T(G_{\{e\}_{2,e_g,m;o}, 1, y) = (e_1 + e_2 + y - 1)^m . \quad (3.20)$$

and

$$\begin{aligned} T(G_{\{e\}_{r=2,e_g,m;c}, 1, y) &= (e_1 + e_2 + y - 1)^{m-1} \times \\ &\times \left[(me_g + y - 1)(e_1 + e_2 + y - 1) + me_1 e_2 \right] . \end{aligned} \quad (3.21)$$

These $r = 2$ results are in agreement with Eqs. (3.1)-(3.4) in [24], which used the notation $p = e_1 + e_2$. For $r = 3$, we have $T(G_{\{e\}_{r=3,e_g,m;o}, 1, y)$ as in Eq. (3.18), and

$$\begin{aligned} T(G_{\{e\}_{r=3,e_g,m;c}, 1, y) &= [\lambda_{T,0;x=1,r=3}]^{m-1} \times \\ &\times \left[(me_g + y - 1)\lambda_{T,0;x=1,r=3} + me_1 e_2 e_3 \right] , \end{aligned} \quad (3.22)$$

with $\lambda_{T,0;x=1,r=3}$ given in Eq. (3.17). Corresponding explicit expressions for $x = 1$ can be obtained in a similar manner for higher values of r from our general formulas for the Tutte polynomials.

IV. POTTS MODEL PARTITION FUNCTIONS

Using Eq. (2.21), we calculate the equivalent Potts model partition functions

$$Z(G_{\{e\}_{r,e_g,m;o}, q, v) = q(\lambda_{Z,0})^m \quad (4.1)$$

and

$$Z(G_{\{e\}_r, e_g, m; c, q, v}) = (\lambda_{Z,0})^m + (q-1)(\lambda_{Z,1})^m, \quad (4.2)$$

where

$$\lambda_{Z,0} = \frac{(q+v)^{e_g}}{q^r} \left[\prod_{j=1}^r \left\{ (q+v)^{e_j} + (q-1)v^{e_j} \right\} + (q-1) \prod_{j=1}^r \left\{ (q+v)^{e_j} - v^{e_j} \right\} \right] \quad (4.3)$$

and

$$\lambda_{Z,1} = \frac{v^{e_g}}{q^r} \left[\prod_{j=1}^r \left\{ (q+v)^{e_j} + (q-1)v^{e_j} \right\} - \prod_{j=1}^r \left\{ (q+v)^{e_j} - v^{e_j} \right\} \right]. \quad (4.4)$$

Note that the j 'th term in the first product in Eqs. (4.3) and (4.4) is $Z(C_{e_j}, q, v)$, where C_n is the n -vertex circuit graph, so

$$\prod_{j=1}^r \left\{ (q+v)^{e_j} + (q-1)v^{e_j} \right\} = \prod_{j=1}^r Z(C_{e_j}, q, v). \quad (4.5)$$

As a consequence of the equality $x = 1 \Rightarrow q = 0$, Eq. (3.5) implies that, for arbitrary $\{e\}_r$ and e_g ,

$$\lambda_{Z,0} = \lambda_{Z,1} \quad \text{at } q = 0. \quad (4.6)$$

We remark on some special cases. For the case of a single hammock graph $H_{\{e\}_r}$, i.e., $m = 1$ and $e_g = 0$, Eq. (4.1) with (4.3) agrees with (Eq. (2.34) of) [27]. For the special case where each hammock graph is $H_{k,r}$ and $v = -1$, Eq. (4.1) with (4.3) agrees with (Eq. (3.7) in) [19]. For a general hammock chain graph with arbitrary m , our calculations in Eqs. (4.1)-(4.4) agree with the results in Refs. [23, 24] for the $r = 2$ case considered in those studies.

As in the case of the Tutte polynomials, one can express these results in a form with the r -fold products in Eqs. (4.3) and (4.4) multiplied out. Using the same notation as before, we have

$$\begin{aligned} \lambda_{Z,0} = & \frac{(q+v)^{e_g}}{q^{r-1}} \left[(q+v)^{(\sum e_j)_r} + \theta(r-3)a \sum_{\binom{r}{2} \text{ terms}} v^{(\sum e_j)_2} (q+v)^{(\sum e_{j'})_{r-2}} \right. \\ & \left. + \theta(r-4)aD_3 \sum_{\binom{r}{3} \text{ terms}} v^{(\sum e_j)_3} (q+v)^{(\sum e_{j'})_{r-3}} + \dots + aD_r v^{(\sum e_j)_r} \right] \quad (4.7) \end{aligned}$$

and

$$\begin{aligned}
\lambda_{Z,1} = & \frac{v^{e_g}}{q^{r-1}} \left[\theta(r-2) D_2 \sum_{r \text{ terms}} v^{(\sum e_j)_1} (q+v)^{(\sum e_{j'})_{r-1}} \right. \\
& + \theta(r-3) D_3 \sum_{\binom{r}{2} \text{ terms}} v^{(\sum e_j)_2} (q+v)^{(\sum e_{j'})_{r-2}} \\
& \left. + \theta(r-4) D_4 \sum_{\binom{r}{3} \text{ terms}} v^{(\sum e_j)_3} (q+v)^{(\sum e_{j'})_{r-3}} + \dots + D_{r+1} v^{(\sum e_j)_r} \right], \tag{4.8}
\end{aligned}$$

where in terms of the form $v^{(\sum e_j)_d} (q+v)^{(\sum e_{j'})_{r-d}}$, the edges in the sums $(\sum e_j)_d$ and $(\sum e_{j'})_{r-d}$ in the first and second exponents are orthogonal subsets of the full set of edges $\{e\}_r$.

We display the explicit evaluations of these general formulas for the cases $r = 2$ and $r = 3$. For $r = 2$,

$$\lambda_{Z,0} = q^{-1} (q+v)^{e_g} \left[(q+v)^{e_1+e_2} + (q-1)v^{e_1+e_2} \right] \tag{4.9}$$

$$\lambda_{Z,1} = q^{-1} v^{e_g} \left[v^{e_1} (q+v)^{e_2} + v^{e_2} (q+v)^{e_1} + (q-2)v^{e_1+e_2} \right], \tag{4.10}$$

in agreement with Eqs. (4.3) and (4.4) in [24]. For $r = 3$,

$$\begin{aligned}
\lambda_{Z,0} = & q^{-2} (q+v)^{e_g} \left[(q+v)^{e_1+e_2+e_3} \right. \\
& + (q-1) \left\{ v^{e_1+e_2} (q+v)^{e_3} + v^{e_1+e_3} (q+v)^{e_2} + v^{e_2+e_3} (q+v)^{e_1} \right\} \\
& \left. + (q-1)(q-2)v^{e_1+e_2+e_3} \right] \tag{4.11}
\end{aligned}$$

and

$$\begin{aligned}
\lambda_{Z,1} = & q^{-2} v^{e_g} \left[\left\{ v^{e_1} (q+v)^{e_2+e_3} + v^{e_2} (q+v)^{e_1+e_3} + v^{e_3} (q+v)^{e_1+e_2} \right\} \right. \\
& + (q-2) \left\{ v^{e_1+e_2} (q+v)^{e_3} + v^{e_1+e_3} (q+v)^{e_2} + v^{e_2+e_3} (q+v)^{e_1} \right\} \\
& \left. + (q^2 - 3q + 3)v^{e_1+e_2+e_3} \right]. \tag{4.12}
\end{aligned}$$

In a similar manner, one can use our general formulas (4.3) and (4.4), or equivalently, (4.7) and (4.8) to obtain explicit expressions for $\lambda_{Z,0}$ and $\lambda_{Z,1}$ for higher values of r .

The fact that $Z(G, q, v)$ is a polynomial in q (as well as v) for any graph G implies that the expressions in square brackets in Eqs. (4.7) and (4.8) each contain a factor q^{r-1} that

cancels the prefactor $q^{-(r-1)}$ in these expressions. By taking the limit $q \rightarrow 0$, one sees that this implies the identities

$$1 + (q - 1) \sum_{j=2}^r \binom{r}{j} D_j = q^{r-1} \quad (4.13)$$

and

$$\sum_{j=1}^r \binom{r}{j} D_{1+j} = q^{r-1} . \quad (4.14)$$

If $q = 1$, then an elementary result for any graph G is that

$$Z(G, q = 1, v) = e^{Ke(G)} = (v + 1)^{e(G)} . \quad (4.15)$$

We remark on the limits of infinite and zero temperature. The infinite-temperature limit is $\beta \rightarrow 0$, whence also $K = \beta J \rightarrow 0$ and $v \rightarrow 0$. In this limit, for an arbitrary graph, $Z(G, q, v = 0) = q^{n(G)}$, as in Eq. (2.20). This is evident from the cluster representation and has the physical significance that in this limit the Boltzmann factor $e^{-\beta \mathcal{H}} = 1$, so the partition function just enumerates the total set of possible spin configurations, which is $q^{n(G)}$. It is easy to check that the above results satisfy Eq. (2.20), since

$$\lambda_{Z,0} = q^{(\sum_{j=1}^r e_j) + e_g - (r-1)} \quad \text{at } v = 0 \quad (4.16)$$

and

$$\lambda_{Z,1} = 0 \quad \text{at } v = 0 , \quad (4.17)$$

so for the open and cyclic hammock chain graphs,

$$\begin{aligned} Z(G_{\{e\}_{r,e_g,m;o}}, q, v = 0) &= q(\lambda_{Z,0})^m = q^{m[(\sum_{j=1}^r e_j) + e_g - (r-1)] + 1} \\ &= q^{n(G_{\{e\}_{r,e_g,m;o}})} \end{aligned} \quad (4.18)$$

and

$$\begin{aligned} Z(G_{\{e\}_{r,e_g,m;c}}, q, v = 0) &= (\lambda_{Z,0})^m = q^{m[(\sum_{j=1}^r e_j) + e_g - (r-1)]} \\ &= q^{n(G_{\{e\}_{r,e_g,m;c}})} . \end{aligned} \quad (4.19)$$

One may also consider the limit of zero temperature. If $J > 0$, i.e., the spin-spin interaction is ferromagnetic, then as $T \rightarrow 0$, i.e., $K = \beta J \rightarrow +\infty$ (and thus also $v \rightarrow \infty$), the spins are all aligned in one of the q states of the Potts model, so for an arbitrary graph G ,

$$\lim_{v \rightarrow \infty} Z(G, q, v) = q \exp[Ke(G)] , \quad (4.20)$$

where $e(G)$ denotes the number of edges of G . Again, in addition to the physical explanation, this is evident from the cluster representation (2.18). One checks that our calculations for the open and cyclic hammock chain graphs satisfy this general result as follows. Here the terms $\lambda_{Z,0}$ and $\lambda_{Z,1}$ have the same limiting form:

$$\lambda_{Z,0} \rightarrow v^{(\sum_{j=1}^r e_j)+e_g} \rightarrow \exp \left[K \left(\left(\sum_{j=1}^r e_j \right) + e_g \right) \right] \quad \text{as } K \rightarrow \infty \quad (4.21)$$

and

$$\lambda_{Z,1} \rightarrow v^{(\sum_{j=1}^r e_j)+e_g} \rightarrow \exp \left[K \left(\left(\sum_{j=1}^r e_j \right) + e_g \right) \right] \quad \text{as } K \rightarrow \infty . \quad (4.22)$$

Hence, using Eq. (2.3), one sees that for both open and cyclic boundary conditions,

$$Z(G_{\{e\}_{r,e_g,m;BC}, q, v}) \rightarrow q \exp[K e(G_{\{e\}_{r,e_g,m;BC})] \quad \text{as } K \rightarrow \infty , \quad (4.23)$$

in agreement with the general result (4.20). If $T \rightarrow 0$ with $J < 0$, i.e., $K \rightarrow -\infty$ and $v \rightarrow -1$, one has the identity $Z(G, q, v = -1) = P(G, q)$, as noted above.

V. CHROMATIC POLYNOMIALS

In this section we discuss a particularly interesting special case of the Potts/Tutte polynomials, namely chromatic polynomials (for some background, see, e.g., [5]-[7], [17, 26]). Given the relation (1.4), we make the substitution $v = -1$ in our general results for $Z(G_{\{e\}_{r,e_g,m;o}, q, v})$ and $Z(G_{\{e\}_{r,e_g,m;c}, q, v})$ to obtain the corresponding chromatic polynomials $P(G_{\{e\}_{r,e_g,m;o}, q})$ and $P(G_{\{e\}_{r,e_g,m;c}, q})$. We have

$$P(G_{\{e\}_{r,e_g,m;o}, q}) = q(\lambda_{P,0})^m \quad (5.1)$$

and

$$P(G_{\{e\}_{r,e_g,m;c}, q}) = (\lambda_{P,0})^m + (q-1)(\lambda_{P,1})^m , \quad (5.2)$$

where

$$\begin{aligned} \lambda_{P,0} &= (\lambda_{Z,0})|_{v=-1} \\ &= \frac{(q-1)^{e_g}}{q^r} \left[\left\{ \prod_{j=1}^r P(C_{e_j}, q) \right\} + \frac{1}{(q-1)^{r-1}} \left\{ \prod_{j=1}^r P(C_{e_j+1}, q) \right\} \right] \end{aligned} \quad (5.3)$$

and

$$\begin{aligned}
\lambda_{P,1} &= (\lambda_{Z,1})|_{v=-1} \\
&= \frac{(-1)^{e_g}}{q^r} \left[\left\{ \prod_{j=1}^r P(C_{e_j}, q) \right\} - \frac{1}{(q-1)^r} \left\{ \prod_{j=1}^r P(C_{e_{j+1}}, q) \right\} \right].
\end{aligned} \tag{5.4}$$

We will synonymously use the short-form notation $\lambda_{P,0}$ and $\lambda_{P,1}$ as in Eqs. (5.3) and (5.4) and, where necessary for clarity, the long-form notation $\lambda_{P,0;\{e\}_r,e_g}$ and $\lambda_{P,1;\{e\}_r,e_g}$. The poles at $q = 0$ and $q = 1$ in various prefactors in Eqs. (5.3) and (5.4) are cancelled by factors arising from the polynomials $P(C_{e_j}, q)$ and $P(C_{e_{j+1}}, q)$ in the r -fold products. This cancellation is rendered explicit by the use of the factorization in Eq. (2.29) with (2.30) to express $\lambda_{P,0}$ and $\lambda_{P,1}$ in terms of the D_{e_j} and $D_{e_{j+1}}$ polynomials, yielding

$$\lambda_{P,0} = (q-1)^{e_g} \left[(q-1)^r \left\{ \prod_{j=1}^r D_{e_j} \right\} + (q-1) \left\{ \prod_{j=1}^r D_{e_{j+1}} \right\} \right] \tag{5.5}$$

and

$$\lambda_{P,1} = (-1)^{e_g} \left[(q-1)^r \left\{ \prod_{j=1}^r D_{e_j} \right\} - \left\{ \prod_{j=1}^r D_{e_{j+1}} \right\} \right]. \tag{5.6}$$

The special case $m = 1$ and $e_g = 0$ corresponds to a single hammock graph, $H_{\{e\}_r}$. In this special case, one has

$$\begin{aligned}
P(H_{\{e\}_r}, q) &= \frac{1}{q^{r-1}} \left[\left\{ \prod_{j=1}^r P(C_{e_j}, q) \right\} + \frac{1}{(q-1)^{r-1}} \left\{ \prod_{j=1}^r P(C_{e_{j+1}}, q) \right\} \right] \\
&= q(q-1) \left[(q-1)^{r-1} \left\{ \prod_{j=1}^r D_{e_j} \right\} + \left\{ \prod_{j=1}^r D_{e_{j+1}} \right\} \right].
\end{aligned} \tag{5.7}$$

In general, the minimum value of q for which one can perform a proper q -coloring of a graph G is the chromatic number, $\chi(G)$. For the hammock graphs, $\chi(G_{\{e\}_r,e_g,m,BC})$ is 2 if all circuits on $G_{\{e\}_r,e_g,m,BC}$ are of even length, and 3 otherwise. We recall that the zeros of a chromatic polynomial $P(G, q)$ are called the chromatic zeros of the graph G . These always include $q = 0$ and for a graph with at least one edge, also $q = 1$. Thus,

$P(G_{\{e\}_r, e_g, m, BC}, q)$ always contains a factor $q(q-1)$. If $G_{\{e\}_r, e_g, m, BC}$ contains a circuit of odd length, then $P(G_{\{e\}_r, e_g, m, BC}, q)$ also contains a factor $(q-2)$ and hence vanishes at $q=2$. It is straightforward to derive this property from the analytic results given above for $\lambda_{P,0}$ and $\lambda_{P,1}$. Let us consider first the case of an open hammock chain and observe that at $q=2$, $D_k = 1$ if k is even and $D_k = 0$ if k is odd (cf. Eq. (17.4)). If all $e_j \in \{e\}_r$ are even, then $\left[\prod_{j=1}^r D_{e_j}\right]_{q=2} = 1$, while $\left[\prod_{j=1}^r D_{e_{j+1}}\right]_{q=2} = 0$, so, from Eq. (5.1), it follows that $P(G_{\{e\}_r, e_g, m; 0}, q) = 2(\lambda_{P,0})^m$ has the following values at $q=2$:

$$P(G_{\{e\}_r, e_g, m; 0}, 2) = \begin{cases} 2 & \text{if } e_j \in \{e\}_r \text{ are all even or all odd} \\ 0 & \text{if } \{e\}_r \text{ contains both even and odd edges} \end{cases} . \quad (5.8)$$

Next, let us consider the cyclic hammock chain. Here we observe that at $q=2$, $P(G_{\{e\}_r, e_g, m; c}, 2) = (-1)^{e_g} [(\lambda_{P,0})^m - (\lambda_{P,1})^m]$. Now, with $q=2$, if all $e_j \in \{e\}_r$ are even, then $\lambda_{P,1} = (-1)^{e_g}$, while if all $e_j \in \{e\}_r$ are odd, then $\lambda_{P,1} = -(-1)^{e_g}$, and if the set $\{e\}_r$ contains both even and odd edges, then $\lambda_{P,1} = 0$. So for this cyclic hammock chain, the chromatic polynomial $P(G_{\{e\}_r, e_g, m; c}, q)$ evaluated at $q=2$, has the following values:

$$\text{all } e_j \text{ even} \Rightarrow P(G_{\{e\}_r, e_g, m; c}, 2) = 1 + (-1)^{me_g} = \begin{cases} 2 & \text{if } me_g \text{ is even} \\ 0 & \text{if } me_g \text{ is odd} \end{cases} \quad (5.9)$$

while

$$\text{all } e_j \text{ odd} \Rightarrow P(G_{\{e\}_r, e_g, m; c}, 2) = 1 + (-1)^{m(e_g+1)} = \begin{cases} 2 & \text{if } m(e_g+1) \text{ is even} \\ 0 & \text{if } m(e_g+1) \text{ is odd} \end{cases} . \quad (5.10)$$

Finally,

$$P(G_{\{e\}_r, e_g, m; c}, 2) = 0 \text{ if } \{e\}_r \text{ contains both even and odd } e_j . \quad (5.11)$$

These analytic results are in accord with the general statement above that $P(G_{\{e\}_r, e_g, m; 0}, 2)$ and $P(G_{\{e\}_r, e_g, m; c}, 2)$ vanish whenever the respective graph contains a circuit of odd length. For an arbitrary graph G , the property that $P(G, 2) = 2$ is equivalent to the property that G is bipartite.

As noted in the Introduction, a feature of particular interest here is that for sufficiently large q on a given graph G with finite maximal vertex degree, the zero-temperature Potts antiferromagnet has a nonzero entropy per vertex, $S_0 = k_B \ln W$, or equivalently, a configurational degeneracy per vertex W that is greater than unity. Here, for a finite graph G , W

is given by

$$W(G, q) = [P(G, q)]^{1/n(G)} , \quad (5.12)$$

and thus, in the $n \rightarrow \infty$ limit,

$$W(\{G\}, q) = \lim_{n(G) \rightarrow \infty} P(G, q)^{\frac{1}{n(G)}} . \quad (5.13)$$

As discussed in [20, 31], for certain values of q , denoted q_s , one must take account of the noncommutativity

$$\lim_{n(G) \rightarrow \infty} \lim_{q \rightarrow q_s} [P(G, q)]^{1/n(G)} \neq \lim_{q \rightarrow q_s} \lim_{n(G) \rightarrow \infty} [P(G, q)]^{1/n(G)} . \quad (5.14)$$

The special values of q_s here include $q \in \{0, 1\}$, since $P(G_{\{e\}_r, e_g, m; BC}, q)$ vanishes at these values and also the value $q = 2$ if $G_{\{e\}_r, e_g, m; BC}$ contains a circuit with an odd number of edges.

VI. CHROMATIC ZEROS, THEIR ACCUMULATION LOCUS IN THE L_m LIMIT, AND GROUND STATE DEGENERACY W

A. General

We next discuss the zeros of the chromatic polynomials of the open and cyclic hammock chain graphs and their continuous accumulation locus in the limit of infinite chain length, $m \rightarrow \infty$, with fixed r , $\{e\}_r$, and e_g , denoted L_m limit in Section II. For an arbitrary graph G , the coefficients of powers of q in $P(G, q)$ are real (actually, integers), and hence the set of zeros of $P(G, q)$ in the q plane is invariant under complex conjugation. The chromatic zeros of the open hammock chain, $G_{\{e\}_r, e_g, m; o}$ are discrete and do not form a continuous locus in the q plane in the L_m limit. In contrast, in this L_m limit, almost all of the chromatic zeros for the cyclic hammock chain graph $G_{\{e\}_r, e_g, m; c}$ merge to form a continuous locus, denoted \mathcal{B} , consisting of one or more closed curves in the q plane. As in [20] and subsequent works, here the symbol \mathcal{B} stands for “boundary”. Henceforth, in our discussion of \mathcal{B} , we implicitly restrict to the case of cyclic boundary conditions. Properties of chromatic zeros in the case of a single hammock graph $H_{\{e\}_r}$ were discussed in [19, 23, 27, 28]; in particular, it was shown in [19] that in the L_r limit, these zeros have unbounded magnitude, they do merge to form a nontrivial continuous locus comprised of curves, and this locus passes through the origin of the $1/q$ plane. Here we restrict to the L_m limit. As a preface to the discussion below,

it is useful to recall that for an arbitrary graph, a chromatic polynomial has the following zero-free regions on the real axis: (i) $(-\infty, 0)$, (ii) $(0,1)$ [32], and (iii) $(1, \frac{32}{27})$ [7, 33, 34].

The location of the continuum accumulation set of chromatic zeros in the L_m limit is determined by an application of a theorem due to Beraha, Kahane, and Weiss (BKW) [35, 36]. For values of q where $\lambda_{P,0}$ and $\lambda_{P,1}$ are both nonzero, the locus \mathcal{B} occurs where

$$|\lambda_{P,0}| = |\lambda_{P,1}| . \quad (6.1)$$

This is easily understood, since, as is evident in Eq. (5.2), $P(G_{\{e\}_{r,e_g,m;c}}, q)$ is a sum of m 'th powers of $\lambda_{P,0}$ and $\lambda_{P,1}$, so in order to have a cancellation between these terms yielding a zero in this chromatic polynomial, it is necessary that they should have the same magnitude. The situation where $\lambda_{P,0} = \lambda_{P,1} = 0$ at a given q requires a more detailed analysis, as was discussed in [23] and is elaborated upon further below. For moderately large values of m , most chromatic zeros lie close to (or on) the asymptotic locus \mathcal{B} . For a given limit $\{G\}$, the maximal point at which \mathcal{B} intersects the real axis is denoted $q_c = q_c(\{G\})$. In passing, we note that an isolated chromatic zero not on \mathcal{B} for $\{G_{\{e\}_{r,e_g;c}}\}$ is the zero at $q = 1$. For an arbitrary graph, since the set of zeros of $P(G, q)$ is invariant under complex conjugation $q \rightarrow q^*$, it follows that the continuous accumulation locus \mathcal{B} is also invariant under complex conjugation: $\mathcal{B}^* = \mathcal{B}$. The locus \mathcal{B} is an algebraic curve, in the terminology of algebraic geometry. We recall that a multiple point (MP) on an algebraic curve is defined as a point where several branches of the curve intersect [37, 38]. If there are n_i branches intersecting at a multiple point, and if these have different tangents at the intersection point, then the multiple point is said to have index n_i . In this case, $2n_i$ curves emanate out from the multiple point (or, equivalently, go into it), forming the n_i branches. As one crosses a curve on \mathcal{B} (away from possible multiple points), there is a switching between dominant terms λ ; for the cyclic hammock chain graphs there are just two such λ terms contributing to the chromatic polynomial (5.2), namely $\lambda_{P,0}$ and $\lambda_{P,1}$ in Eqs. (5.3) and (5.4). Correspondingly, there is nonanalytic change in the W function, as discussed below.

An important question concerning the Potts antiferromagnet on the $n \rightarrow \infty$ limit of a given family of graphs is the form of this locus \mathcal{B} and, in particular, the value of q_c . On a graph with vertices of bounded degree, for sufficiently large (real) q , $W(\{G\}, q) \sim q$. As q decreases through (real) positive values, $W(\{G\}, q)$ first changes its analytic form as q decreases through q_c , crossing the boundary \mathcal{B} . As in earlier works such as [20, 23], we denote the region in the complex q plane that is analytically connected with the line segment $q > q_c$ as region R_1 . In the evaluation of Eq. (5.13), there are actually $n(G)$ different $1/n(G)$ 'th roots of $P(G, q)$. To ensure that $W(\{G\}, q)$ is real and nonnegative in physical applications, one picks the canonical real positive root for real positive $q > q_c$. In contrast, in regions not

analytically connected with R_1 , there is no canonical choice of root to take in Eq. (5.13), so one can only determine the magnitude $|W(\{G\}, q)|$ [20]. From our general calculations, for the L_m limit of a cyclic hammock chain and for $q \in R_1$, where $\lambda_{P,0}$ is dominant, we have

$$W(\{G_{\{e\}_r, e_g; c}\}, q) = [\lambda_{P,0; \{e\}_r, e_g}]^{\frac{1}{[(\sum_{j=1}^r e_j) + e_g + (r-1)]}} \quad \text{for } q \in R_1 . \quad (6.2)$$

As noted above, when one crosses a generic point on a curve on the boundary locus \mathcal{B} away from any possible multiple points, there is a switch in the dominant λ in the chromatic polynomial (5.2). Thus, crossing \mathcal{B} from the region R_1 away from a multiple point, and entering another region, denoted generically as R_x , the dominant λ in this other region is $\lambda_{P,1}$, so

$$W(\{G_{\{e\}_r, e_g; c}\}, q) = [\lambda_{P,1; \{e\}_r, e_g}]^{\frac{1}{[(\sum_{j=1}^r e_j) + e_g + (r-1)]}} \quad \text{for } q \in R_x . \quad (6.3)$$

In both Eqs. (6.2) and (6.3), we take the limit $n(G) \rightarrow \infty$ first and then $q \rightarrow q_s$, where q_s denotes the special points mentioned in connection with the noncommutativity (5.14).

If one crosses the locus \mathcal{B} at a multiple point and enters one of the loop regions connected to this multiple point (e.g. at any of the three multiple points on the locus \mathcal{B} for the $r = 2$ family $(\{e_1, e_2\}, e_g) = (\{4, 4\}, 0)$ in Fig. 2, the dominant λ in the loop region is still $\lambda_{P,0}$, as is true for the two loop regions connected to the multiple point at $q = 2$ on the locus \mathcal{B} for the $r = 3$ family $(\{e_1, e_2, e_3\}, e_g) = (\{2, 2, 2\}, 0)$ in Fig. 7. This property was noted for $r = 2$ in [23], and our results with higher r again exhibit the same property. Thus, as will be discussed below, when one increases e_g from 0 to nonzero values and these loop regions connected to multiple points on \mathcal{B} separate to form bubble regions, the dominant λ in these bubble regions continues to be $\lambda_{P,1}$. Let us denote the number of regions bounded by components of \mathcal{B} , by $N_{\text{reg.}}$ and the number of disjoint components on \mathcal{B} as $N_{\text{comp.}}$. For families where the respective loci \mathcal{B} do not contain any multiple points, $N_{\text{comp.}}$ and $N_{\text{reg.}}$ are simply related by [23]

$$N_{\text{reg.}} = N_{\text{comp.}} + 1 \quad \text{if no multiple point on } \mathcal{B} . \quad (6.4)$$

As was discussed in [19, 23], for a given family of graphs, e.g., the $r = 2$ cyclic hammock graphs with loci \mathcal{B} not containing any multiple point(s), there is an upper bound on $N_{\text{comp.}}$ from the Harnack theorem in algebraic geometry [38, 39]. However, as shown in [23], it is not very restrictive; for the simplest $r = 2$ case, $(\{e_1, e_2\}, e_g) = (\{2, 2\}, 1)$, this bound is $N_{\text{comp.}} \leq 37$, while the actual number is $N_{\text{comp.}} = 2$. As e_g increases in this $(\{2, 2\}, e_g)$ family, the Harnack upper bound increases above 37, but $N_{\text{comp.}}$ remains equal to 2 and hence is even less restrictive. This assessment in [23] also applies to families of cyclic hammock graphs with higher r . Parenthetically, we note that the Harnack upper bound is known to be sharp; i.e., there exist curves (different from those considered in this study) that saturate it [39].

With regard to the boundary locus \mathcal{B} , first, if $r = 1$, then $G_{e_1, e_g, m; c}$ is just the circuit graph with $n = m(e_1 + e_g)$ vertices, so \mathcal{B} is the unit circle $|q - 1| = 1$ in the complex q plane and $q_c = 2$. Henceforth, we restrict to the cases where $r \geq 2$. In Ref. [23] a number of general results were proved for \mathcal{B} for the $r = 2$ case considered there. These included the following:

- (B1) \mathcal{B} is compact.
- (B2) \mathcal{B} passes through $q = 0$ as the most leftward crossing on the real q axis.
- (B3) \mathcal{B} encloses regions in the q plane.
- (B4) (with the ordering $e_1 \leq e_2$) if $e_1 = 1$, then \mathcal{B} is the unit circle $|q - 1| = 1$ independent of the values of e_2 and e_g ; thus, in this case, $q_c = 2$. The chromatic zeros of $G_{\{e_1, e_2\}, e_g, m}$ (aside from the discrete zero at $q = 1$) lie exactly on this locus for general e_2 , e_g , and m .
- (B5) if $p = e_1 + e_2$ is even, then $q_c = 2$.
- (B6) if p is odd and $e_1 \geq 2$, then $q_c < 2$ and for fixed (e_1, e_2) , q_c increases monotonically as e_g increases, approaching 2 from below as $e_g \rightarrow \infty$.

We find that properties (B1), (B2), and (B3) also hold for general r and are proved in the same way as for the $r = 2$ case. Each region is bounded by a component of the total boundary \mathcal{B} . Concerning the property (B2), we find that as q increases from negative real values through $q = 0$ to small positive values, the dominant λ switches from $\lambda_{P,0}$ to $\lambda_{P,1}$. As in [23], we denote the region that is contiguous with region R_1 at $q = 0$ as R_2 . This region R_2 contains the discrete zero at $q = 1$.

There is also a generalization of property (B4). As a step in the proof of (B4), Ref. [23] showed (with the given ordering $e_1 \leq e_2$) that if $e_1 = 1$, then the chromatic polynomial for the cyclic polygon chain reduces to

$$P(G_{\{e\}_{r=2, e_g, m; c}}, q) = (D_{e_1 + e_2})^m P(C_{n_c}, q) = q(q - 1)(D_{1 + e_2})^m D_{n_c}, \quad (6.5)$$

where

$$n_c = m(e_1 + e_g) = m(1 + e_g). \quad (6.6)$$

The subscript c indicates that in this $e_1 = 1$ case, there is a global circuit formed as one traverses a route along the edge e_1 of a given $r = 2$ hammock (polygon), then the e_g edges, then the e_1 edge of the next polygon, and so forth, returning to the starting vertex after a

length of n_c vertices, equal to the same number of edges. This is the origin of the product factor $P(C_{n_c}, q)$ in the reduction formula (6.5). The result then follows, since \mathcal{B} is determined by the behavior of the zeros of $P(C_{n_c}, q)$, and is the unit circle $|q - 1| = 1$ in the complex q plane. Aside from the discrete zero at $q = 1$, the zeros of $P(C_{n_c}, q)$ lie exactly on this locus.

Here we generalize property (B4) to arbitrary r . The case $r = 1$ has already been discussed above and for that case \mathcal{B} is the unit circle $|q - 1| = 1$ for arbitrary e_1 and e_g . We thus focus on the cases $r \geq 2$. Again using our standard ordering of edge values $e_1 \leq e_2 \leq \dots \leq e_r$, we find that if $e_1 = 1$, then $P(G_{\{e\}r, e_g, m; c}, q)$ reduces as

$$P(G_{\{e\}r, e_g, m; c}, q) = \left[\prod_{j=2}^r D_{1+e_j} \right]^m P(C_{n_c}, q) = q(q-1) \left[\prod_{j=2}^r D_{1+e_j} \right]^m D_{n_c}, \quad (6.7)$$

where each factor D_{1+e_j} can equivalently be written $D_{e_1+e_j}$. Thus, the same result follows for \mathcal{B} for general r as for $r = 2$ (and $r = 1$), namely that in this case, \mathcal{B} is the unit circle $|q - 1| = 1$ in the complex q plane.

B. Determination of q_c

The locus \mathcal{B} crosses the real q axis at a left-most point, $q = 0$, and a right-most point, q_c . In this section we determine q_c . This involves generalizing the properties (B5) and (B6) presented for the $r = 2$ case in Ref. [23]. We find that, depending on the edge parameters $\{e\}_r$ and e_g , q_c is at most 2, so one part of the analysis consists of determining the conditions under which it is equal to 2. Since if $\min(e_j) = 1$, then \mathcal{B} is fully determined to be the circle $|q - 1| = 1$, and hence $q_c = 2$, the only cases that we need to consider are those with $e_j \geq 2$ for all $j = 1, \dots, r$.

It is instructive first to review the situation for $r = 2$ studied in [23] (which used the notation $a_1 = \lambda_{P,0}$ and $a_2 = \lambda_{P,1}$); here, $\lambda_{P,0}$ and $\lambda_{P,1}$ are :

$$\lambda_{P,0;r=2} = (q-1)^{e_g+1} D_{e_1+e_2} \quad (6.8)$$

and

$$\lambda_{P,1;r=2} = (-1)^{e_1+e_2+e_g} q^{-1} \left[(1-q)^{e_1} + (1-q)^{e_2} + q - 2 \right]. \quad (6.9)$$

In this $r = 2$ case, if $q = 2$ (as indicated in the subscript), then

$$\lambda_{P,0;\{e\}r=2, e_g, q=2} = \begin{cases} 1 & \text{if } e_1 + e_2 \text{ is even} \\ 0 & \text{if } e_1 + e_2 \text{ is odd} \end{cases} \quad (6.10)$$

and

$$\lambda_{P,1;\{e\}_{r=2,e_g,q=2}} = \begin{cases} (-1)^{e_g} & \text{if } e_1 \text{ and } e_2 \text{ are both even} \\ -(-1)^{e_g} & \text{if } e_1 \text{ and } e_2 \text{ are both odd} \\ 0 & \text{if } e_1 + e_2 \text{ is odd} \end{cases} . \quad (6.11)$$

In analyzing whether a special (sp) point denoted q_{sp} is on \mathcal{B} , the criterion $|\lambda_{P,0}| = |\lambda_{P,1}|$ suffices if these are both nonzero at q_{sp} , but if they are both zero at this point, then one must examine the Taylor series expansions of $\lambda_{P,0}$ and $\lambda_{P,1}$ around this point. If the respective leading terms in these expansions for $\lambda_{P,0}$ and $\lambda_{P,1}$ occur at the same order $O((q - q_{sp})^t)$ and have coefficients of $(q - q_{sp})^t$ that are equal in magnitude, then q_{sp} is on the locus \mathcal{B} . If they occur at different orders, or at the same order with coefficients of different magnitudes, then as $m \rightarrow \infty$ and $q \rightarrow 2$, the contribution of the smaller term in the set $\{(\lambda_{P,0})^m, (\lambda_{P,1})^m\}$ becomes negligibly small compared with the contribution from the larger one, precluding any possibility of a cancellation that could lead to a zero in the chromatic polynomial and hence implying that the point $q = 2$ is not on \mathcal{B} , which is the continuous accumulation set of these zeros. As indicated in Eqs. (6.10) and (6.11), in the $r = 2$ case considered in [23], if one of the set $\{e_1, e_2\}$ is odd and the other is even, then $\lambda_{P,0} = \lambda_{P,1} = 0$ at $q = 2$. The Taylor series expansions for this case are [23]

$$\lambda_{P,0;\{e\}_{r=2,e_g}} = \frac{1}{2}(e_1 + e_2 - 1)(q - 2) + \dots \quad \text{as } q \rightarrow 0 \quad (6.12)$$

and

$$\lambda_{P,1;\{e\}_{r=2,e_g}} = \frac{(-1)^{e_g+1}}{2}(1 + e_{\text{even}} - e_{\text{odd}})(q - 2) + \dots , \quad (6.13)$$

where, for clarity, we indicate the parameters as subscripts; e_{even} and e_{odd} refer to whichever of the set $\{e_1, e_2\}$ are even and odd; and $+\dots$ indicates higher-order terms in the respective Taylor series expansions. As discussed in [23], since

$$\frac{|1 + e_{\text{even}} - e_{\text{odd}}|}{e_1 + e_2 - 1} < 1 \quad (6.14)$$

for the relevant case where $\min(e_j) \geq 2$, it follows that for this situation in which $e_1 + e_2$ is odd, the point $q = 2$ is not on \mathcal{B} . Since $|\lambda_{P,0}| > |\lambda_{P,1}|$ for (real) $q > 2$, it also follows that $q_c < 2$ in this case; the actual value of q_c depends on e_1 , e_2 , and e_g . Illustrative plots showing \mathcal{B} for $e_1 = 2$, $e_2 = 3$, and $0 \leq e_g \leq 3$ were included as Figs. 3(a,b) and 4(a,b) in [23]. For $e_1 = 2$, $e_2 = 3$, and $e_g = 0, 1, 2$, q_c has the respective values (given to the indicated floating-point precision) 1.453398, 1.569840, 1.636883, which are the unique real solutions to the respective equations

$$q_c(\{(2, 3), 0\}) : \quad q^3 - 3q^2 + 5q - 4 = 0 , \quad (6.15)$$

$$q_c(\{2, 3, 1\}) : \quad q^3 - 4q^2 + 7q - 5 = 0 , \quad (6.16)$$

and

$$q_c(\{2, 3, 2\}) : \quad q^5 - 5q^4 + 11q^3 - 13q^2 + 9q - 4 = 0 . \quad (6.17)$$

The property that (in this case of odd $e_1 + e_2$) q_c increases toward 2 from below as $e_g \rightarrow \infty$ follows because $\lambda_{P,0}$ contains a factor $(q-1)^{e_g+1}$, while $|\lambda_{P,1}|$ is independent of e_g , so in order for $|\lambda_{P,0}|$ to be equal to $|\lambda_{P,1}|$ as must be true at q_c , it is necessary that $q \nearrow 2$ as $e_g \rightarrow \infty$.

We now generalize this analysis to arbitrary r . For this purpose, we first observe that at $q = 2$, $\lambda_{P,0}$ and $\lambda_{P,1}$ take the respective forms

$$\lambda_{P,0;q=2} = \frac{1}{2^r} \left[\prod_{j=1}^r \{1 + (-1)^{e_j}\} + \prod_{j=1}^r \{1 - (-1)^{e_j}\} \right] \quad (6.18)$$

and

$$\lambda_{P,1;q=2} = \frac{(-1)^{e_g}}{2^r} \left[\prod_{j=1}^r \{1 + (-1)^{e_j}\} - \prod_{j=1}^r \{1 - (-1)^{e_j}\} \right] . \quad (6.19)$$

If all $e_j \in \{e\}_r$ are even, then the first r -fold product in Eqs. (6.18) and (6.19) is 2^r , while the second product is zero. If all $e_j \in \{e\}_r$ are odd, then the first r -fold product in Eqs. (6.18) and (6.19) is zero while the second is 2^r . Therefore if all $e_j \in \{e\}_r$ are even, then $\lambda_{P,0;q=2} = 1$ and $\lambda_{P,1;q=2} = (-1)^{e_g}$, while if all $e_j \in \{e\}_r$ are odd, then $\lambda_{P,0;q=2} = 1$ and $\lambda_{P,1;q=2} = -(-1)^{e_g}$. This shows that if (i) all $e_j \in \{e\}_r$ are even or (ii) all $e_j \in \{e\}_r$ are odd, then $|\lambda_{P,0;q=2}| = |\lambda_{P,1;q=2}| \neq 0$, so the locus \mathcal{B} contains the point $q = 2$, and $q_c = 2$.

If the set of edge values $\{e\}_r$ contains both even and odd members, then both the first and second r -fold products in Eqs. (6.18) and (6.19) vanish, so $\lambda_{P,0;q=2} = \lambda_{P,1;q=2} = 0$, and it is necessary to analyze the Taylor series expansions of these terms around the point $q = 2$ to determine if the point $q = 2$ is on the locus \mathcal{B} . To do this, it is convenient to use a different convention for the ordering of the edge values $e_j \in \{e\}_r$ than the one used in the rest of this paper, namely with $e_1 \leq e_2 \leq \dots \leq e_r$; instead of that convention, here, if there are ℓ odd edges and $r - \ell$ even edges in the set $\{e\}_r$, we order them so that the first ℓ edges are odd, and the remaining $r - \ell$ edges are even. We define

$$\epsilon \equiv q - 2 . \quad (6.20)$$

Substituting $q = 2 + \epsilon$ into the general expressions (5.3) and (5.4) and expanding in powers of ϵ , we obtain the leading-order results

$$\lambda_{P,0} = \frac{1}{2^r} \left[2^{r-\ell} \left\{ \prod_{j=1}^{\ell} (e_j - 1) \right\} \epsilon^\ell + 2^\ell \left(\prod_{j=\ell+1}^r e_j \right) \epsilon^{r-\ell} \right] + \dots \quad (6.21)$$

and

$$\lambda_{P,1} = \frac{(-1)^{e_g}}{2^r} \left[2^{r-\ell} \left\{ \prod_{j=1}^{\ell} (e_j - 1) \right\} \epsilon^\ell - 2^\ell \left(\prod_{j=\ell+1}^r e_j \right) \epsilon^{r-\ell} \right] + \dots \quad (6.22)$$

where, as before, the $+\dots$ indicates higher-order terms in the small quantity ϵ . If $\ell < r - \ell$, i.e., $\ell < r/2$, then the first term in the square brackets in Eqs. (6.21) dominates over the second term, and similarly in Eq. (6.22). We then have, for the leading-order behavior as $q \rightarrow 2$,

$$\lambda_{P,0} = 2^{-\ell} \left\{ \prod_{j=1}^{\ell} (e_j - 1) \right\} \epsilon^\ell + \dots \quad (6.23)$$

and

$$\lambda_{P,1} = 2^{-\ell} (-1)^{e_g} \left\{ \prod_{j=1}^{\ell} (e_j - 1) \right\} \epsilon^\ell + \dots \quad (6.24)$$

Since the leading contributions in the respective Taylor series expansions of $\lambda_{P,0}$ and $\lambda_{P,1}$ around $q = 2$ are equal in magnitude, the point $q = 2$ is on the locus \mathcal{B} and $q_c = 2$. If $\ell > r - \ell$, i.e., $\ell > r/2$, then the second term in the square brackets in Eqs. (6.21) dominates over the first term, and similarly in Eq. (6.22). Hence, the leading-order behavior as $q \rightarrow 2$ is

$$\lambda_{P,0} = 2^{-(r-\ell)} \left(\prod_{j=\ell+1}^r e_j \right) \epsilon^{r-\ell} + \dots \quad (6.25)$$

and

$$\lambda_{P,1} = 2^{-(r-\ell)} (-1)^{e_g+1} \left(\prod_{j=\ell+1}^r e_j \right) \epsilon^{r-\ell} + \dots \quad (6.26)$$

Again, the leading contributions in the respective Taylor series expansions of $\lambda_{P,0}$ and $\lambda_{P,1}$ around $q = 2$ are equal in magnitude, so the point $q = 2$ is on the locus \mathcal{B} and $q_c = 2$.

Finally, if $\ell = r - \ell$, i.e., $r = 2\ell$, then both terms in the square brackets in Eqs. (6.21) for $\lambda_{P,0}$ are of equal order in the small quantity ϵ , as are both terms in Eq. (6.22) for $\lambda_{P,1}$. Hence, in this case, the leading-order behavior as $q \rightarrow 2$ is

$$\lambda_{P,0} = 2^{-\ell} \epsilon^\ell \left[\prod_{j=1}^{\ell} (e_j - 1) + \prod_{j=\ell+1}^{2\ell} e_j \right] + \dots \quad (6.27)$$

and

$$\lambda_{P,1} = 2^{-\ell}(-1)^{e_g}\epsilon^\ell \left[\prod_{j=1}^{\ell} (e_j - 1) - \prod_{j=\ell+1}^{2\ell} e_j \right] + \dots \quad (6.28)$$

Thus, in this case with $r = 2\ell$, the magnitudes of $\lambda_{P,0}$ and $\lambda_{P,1}$ can be expressed concisely as $\lambda_{P,0} = |\lambda_{P,0}| = 2^{-\ell}\epsilon^\ell[A + B]$ and $|\lambda_{P,1}| = 2^{-\ell}\epsilon^\ell|A - B|$, where $A \equiv \prod_{j=1}^{\ell} (e_j - 1)$ and $B \equiv \prod_{j=\ell+1}^{2\ell} e_j$. Since we have excluded zero values for edge(s) $e_j \in \{e\}_r$ (which would lead to spins interacting with themselves in the physical Potts model context), it follows that $A + B > |A - B|$, so $|\lambda_{P,0}| \neq |\lambda_{P,1}|$. Hence, if $r = 2\ell$, i.e., r is even and half of the edges in $\{e\}_r$ are even while the other half are odd, then the point $q = 2$ is not on \mathcal{B} . Furthermore, $\lambda_{P,0} > |\lambda_{P,1}|$ at $q = 2$, which is the same inequality that holds in the region R_1 extending beyond the point $q = 2$ to large positive q . Hence, $q_c < 2$ for this case. The actual value of q_c in this case depends on the values of the edges $\{e\}_r$ and e_g , as was discussed above for $r = 2$. As examples for higher r , we take $r = 4$ and $\{e_1, e_2, e_3, e_4\} = \{2, 2, 3, 3\}$. For $e_g = 0$, $q_c = 1.586793$, while for $e_g = 1$, $q_c = 1.669201$, which are, respectively, the unique real solutions to the equations

$$q_c(\{2, 2, 3, 3\}, 0) : \quad q^5 - 6q^4 + 19q^3 - 36q^2 + 37q - 16 = 0 \quad (6.29)$$

and

$$q_c(\{2, 2, 3, 3\}, 1) : \quad q^5 - 7q^4 + 23q^3 - 42q^2 + 41q - 17 = 0 . \quad (6.30)$$

For the same reason given in the discussion for $r = 2$, as $e_g \rightarrow \infty$ for this case of $r = 2\ell$ with ℓ even and ℓ odd edges in $\{e\}_r$, q_c increases monotonically, approaching 2 from below in this limit. A corollary of this general- r analysis is that the point $q = 2$ is on the locus \mathcal{B} and $q_c = 2$ for the $m \rightarrow \infty$ limit of all cyclic hammock chain graphs $G_{\{e\}_r, e_g, m; c}$ with odd r , while $q = 2$ is not on \mathcal{B} and $q_c < 2$ if r is even. This corollary follows since the equation $\ell = r - \ell$, i.e., $\ell = r/2$ has no integral solution if r is odd.

As an explicit example of these general- r results, we consider the case $r = 3$. Our general results above yield the following expressions for $\lambda_{P,0}$ and $\lambda_{P,1}$ at $q = 2$ (with the values of r and q again indicated with subscripts):

$$\lambda_{P,0; \{e\}_{r=3, e_g; q=2}} = \frac{1}{4} \left[1 + \left\{ (-1)^{e_1+e_2} + (-1)^{e_1+e_3} + (-1)^{e_2+e_3} \right\} \right] \quad (6.31)$$

and

$$\lambda_{P,1; \{e\}_{r=3, e_g; q=2}} = \frac{(-1)^{e_g}}{4} \left[(-1)^{e_1+e_2+e_3} + \left\{ (-1)^{e_1} + (-1)^{e_2} + (-1)^{e_3} \right\} \right] . \quad (6.32)$$

Hence,

- (i) If all of the e_j , $1 \leq j \leq 3$, are even, then $\lambda_{P,0;\{e\}_{r=3,e_g;q=2}} = 1$ and $\lambda_{P,1;\{e\}_{r=3,e_g;q=2}} = (-1)^{e_g}$.
- (ii) If two of the e_j are even and the third is odd, then $\lambda_{P,0;\{e\}_{r=3,e_g;q=2}} = \lambda_{P,1;\{e\}_{r=3,e_g;q=2}} = 0$.
- (iii) If one of the e_j is even and two are odd, then $\lambda_{P,0;\{e\}_{r=3,e_g;q=2}} = \lambda_{P,1;\{e\}_{r=3,e_g;q=2}} = 0$.
- (iv) If all of the e_j are odd, then $\lambda_{P,0;\{e\}_{r=3,e_g;q=2}} = 1$ and $\lambda_{P,1;\{e\}_{r=3,e_g;q=2}} = -(-1)^{e_g}$.

Thus, in accord with our general- r analysis above, if all of the edge values in $\{e\}_{r=3} \equiv \{e_1, e_2, e_3\}$ are even, or all of these edges are odd, then $|\lambda_{P,0;\{e\}_{r=3,e_g;q=2}}| = |\lambda_{P,1;\{e\}_{r=3,e_g;q=2}}| \neq 0$, so the point $q = 2$ is on the locus \mathcal{B} and $q_c = 2$. The remaining two cases in which the $\{e_1, e_2, e_3\}$ set contains both even and odd edges are analyzed via a Taylor series expansion. Since that $\lambda_{Z,0}$ and $\lambda_{Z,1}$ are symmetric functions of the r edge values in the set $\{e\}_r$, we will use the notation e_{odd} to denote the single odd edge value in case (ii) and e_{even} to denote the single even edge value in case (iii). We have

$$\text{case (ii)} : \quad \lambda_{P,0;\{e_j\}_{r=3,e_g}} = \frac{1}{2}(e_{\text{odd}} - 1)(q - 2) + \dots \quad (6.33)$$

$$\text{case (ii)} : \quad \lambda_{P,1;\{e_j\}_{r=3,e_g}} = \frac{1}{2}(-1)^{e_g}(e_{\text{odd}} - 1)(q - 2) + \dots \quad (6.34)$$

and

$$\text{case (iii)} : \quad \lambda_{P,0;\{e_j\}_{r=3,e_g}} = \frac{1}{2}e_{\text{even}}(q - 2) + \dots \quad (6.35)$$

$$\text{case (iii)} : \quad \lambda_{P,1;\{e_j\}_{r=3,e_g}} = \frac{1}{2}(-1)^{e_g+1}e_{\text{even}}(q - 2) + \dots \quad (6.36)$$

in agreement with our general- r results in Eqs. (6.23)-(6.26). Hence, in both cases (ii) and (iii) the leading terms in the Taylor series expansions of $\lambda_{P,0}$ and $\lambda_{P,1}$ are equal in magnitude, and therefore in all four case (i)-(iv) for the family of cyclic hammock graphs with $r = 3$, the point $q = 2$ is on the locus \mathcal{B} and $q_c = 2$, in agreement with our general- r analysis above.

VII. LOCI \mathcal{B} FOR CHROMATIC ZEROS

We have calculated the continuous accumulation sets of chromatic zeros \mathcal{B} for the L_m limits of a large number of different cyclic hammock chain graphs $G_{\{e\}_r,e_g,m;c}$ with various $r \geq 2$ and edge sets $(\{e\}_r, e_g)$. This limit is denoted $\{G_{\{e\}_r,e_g;c}\}$, i.e., with outer brackets, as defined in (2.6), and, with the cyclic boundary condition and L_m limit understood implicitly, these will often be denoted simply as $(\{e\}_r, e_g) = (\{e_1, \dots, e_r\}, e_g)$. In Figs. 2-24 we show

some illustrative plots of these loci for some different choices of $(\{e\}_r, e_g)$. Below we will discuss how these results change when v is changed from its value $v = -1$ for the $T = 0$ Potts antiferromagnet, but here we restrict to this $v = -1$ case. Since it was demonstrated in earlier works such as [10, 20, 23], [40]-[51] (for further references, see, e.g., [52]), that when \mathcal{B} is compact, the zeros of $Z(G_m, q, v)$ in the q plane for strips of various families of graphs lie close to (or on) the asymptotic accumulation locus \mathcal{B} for the $n(G) \rightarrow \infty$ limit, it will suffice for our present purposes to display just these loci \mathcal{B} .

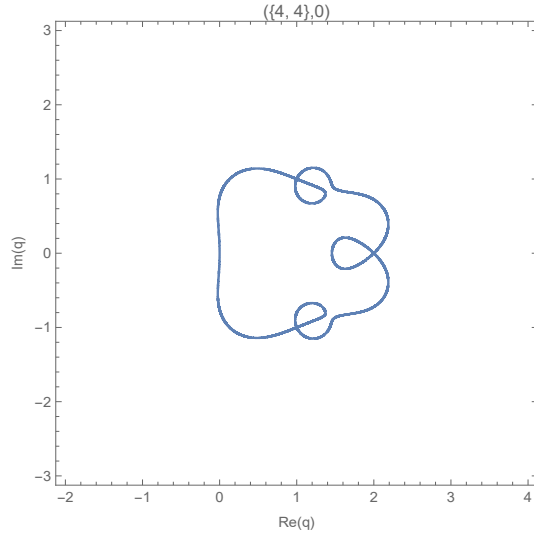


FIG. 2: Locus \mathcal{B} for $r = 2$, $(\{e_1, e_2\}, e_g) = (\{4, 4\}, 0)$.

In the case of the L_m limit of cyclic hammock graphs with $r = 2$, i.e., cyclic polygon chain graphs, it was shown in [23] that if $e_g = 0$, and e_1 and e_2 are both even, then the locus \mathcal{B} has a multiple point (MP) of index 2 at $q = 2$. Ref. [23] also determined the locations of the multiple points for an interesting special $r = 2$ class of cyclic hammock graphs, namely those for which $e_g = 0$ and each of the two ropes have the same number of edges, i.e., $e_1 = e_2 \equiv e_{\text{com}}$:

$$q_\ell = 1 + e^{i\theta_\ell} \quad (7.1)$$

where

$$\theta_\ell = \pm \frac{2\ell\pi}{e_{\text{com}}}, \quad \ell = 0, 1, \dots, \left(\frac{e_{\text{com}} - 2}{2}\right) \quad \text{for } e_{\text{com}} \text{ even} \quad (7.2)$$

$$\theta_\ell = \pm \frac{(2\ell + 1)\pi}{e_{\text{com}}}, \quad \ell = 0, 1, \dots, \left(\frac{e_{\text{com}} - 3}{2}\right) \quad \text{for } e_{\text{com}} \text{ odd}. \quad (7.3)$$

From our calculations of loci \mathcal{B} for cyclic hammock chain graphs with a variety of $r \geq 2$ and edge sets $(\{e\}_r, e_g)$, we find several general features. We begin by describing properties

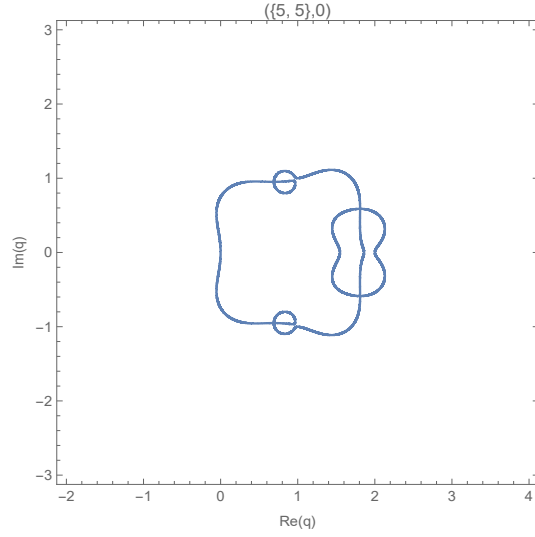


FIG. 3: Locus \mathcal{B} for $r = 2$, $(\{e_1, e_2\}, e_g) = (\{5, 5\}, 0)$.

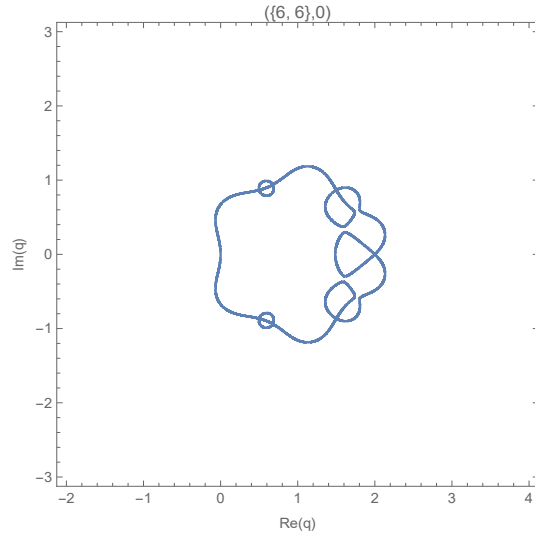


FIG. 4: Locus \mathcal{B} for $r = 2$, $(\{e_1, e_2\}, e_g) = (\{6, 6\}, 0)$.

of the loci for the class of cyclic chain graphs in which all of the edges on the r ropes have the same common value, e_{com} , i.e, $e_j = e_{\text{com}}$ for all $e_j \in \{e\}_r$. This class is denoted as the EJC (e_j -common-value) class. We find the following general properties of \mathcal{B} for this EJC class.

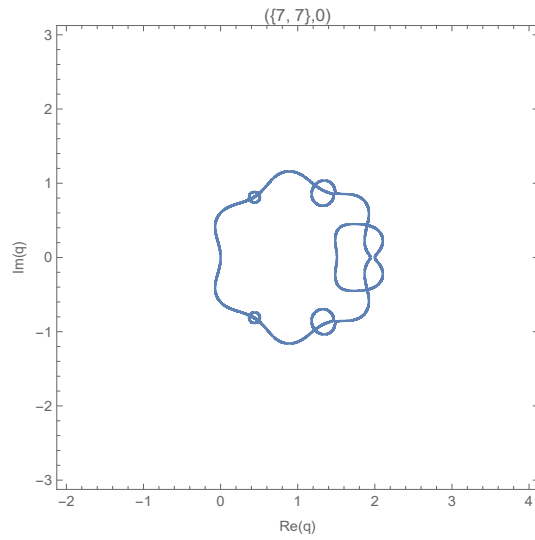


FIG. 5: Locus \mathcal{B} for $r = 2$, $(\{e_1, e_2\}, e_g) = (\{7, 7\}, 0)$.

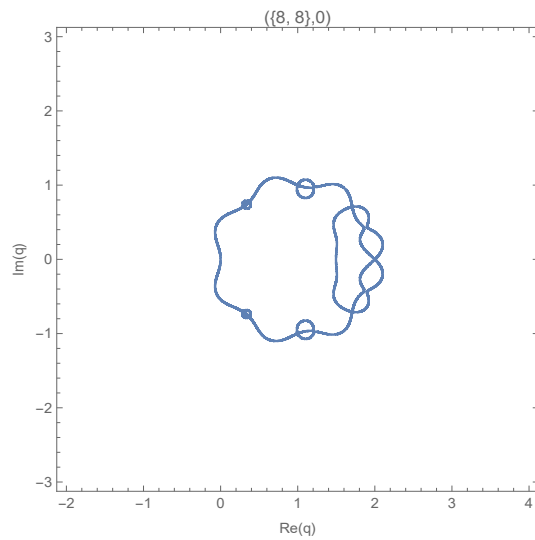


FIG. 6: Locus \mathcal{B} for $r = 2$, $(\{e_1, e_2\}, e_g) = (\{8, 8\}, 0)$.

1. \mathcal{B} passes through $q = 2$ and this point is the maximal point at which it intersects the real q axis, so $q_c = 2$.
2. In this EJC class, a necessary and sufficient condition for \mathcal{B} to have one or more multiple points is that $e_g = 0$. Unless otherwise specified, all of the properties (iii)-(viii) below

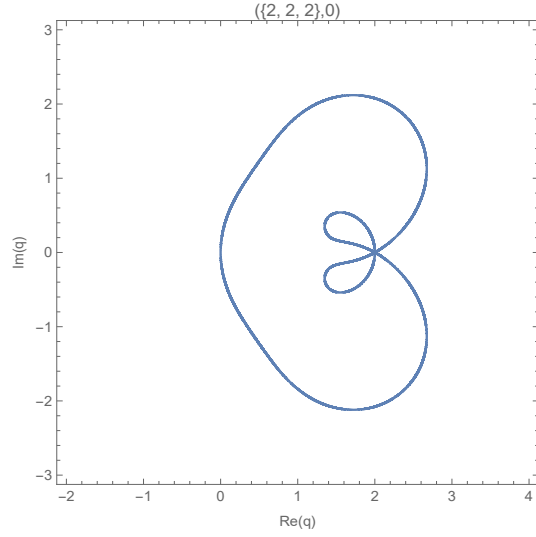


FIG. 7: Locus \mathcal{B} for $r = 3$, $(\{e_1, e_2, e_3\}, e_g) = (\{2, 2, 2\}, 0)$.

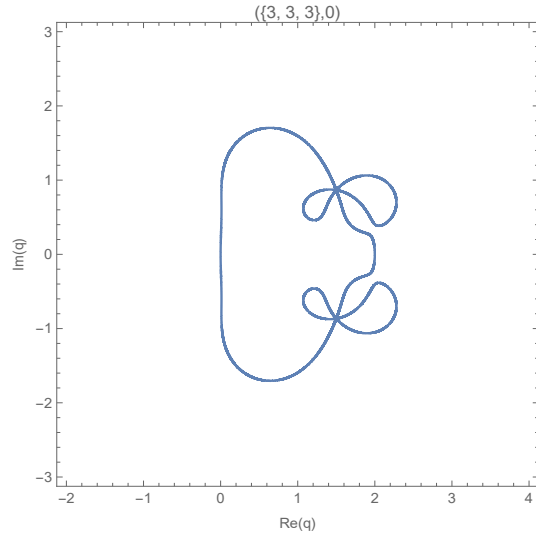


FIG. 8: Locus \mathcal{B} for $r = 3$, $(\{e_1, e_2, e_3\}, e_g) = (\{3, 3, 3\}, 0)$.

assume that this condition $e_g = 0$ is satisfied, in addition to the EJC condition.

3. If $e_g = 0$, then \mathcal{B} has $N_{MP} = e_{\text{com}} - 1$ multiple points. The locations found for these N_{MP} multiple points in [23] for the case $r = 2$ considered there generalize to $r \geq 3$; i.e., they are again given by Eqs. (7.1)-(7.3). A corollary is that, provided $e_g = 0$, one

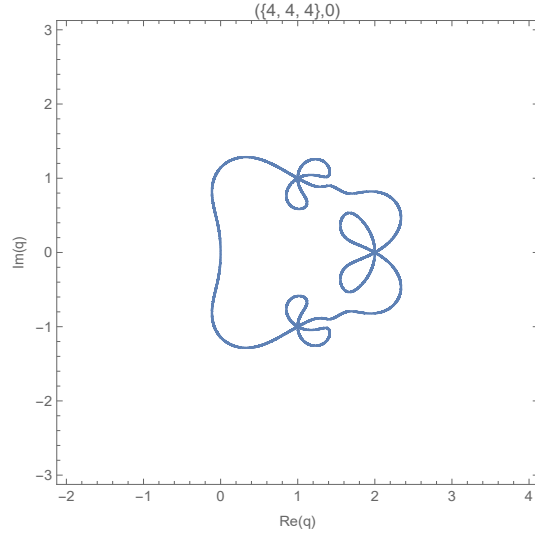


FIG. 9: Locus \mathcal{B} for $r = 3$, $(\{e_1, e_2, e_3\}, e_g) = (\{4, 4, 4\}, 0)$.

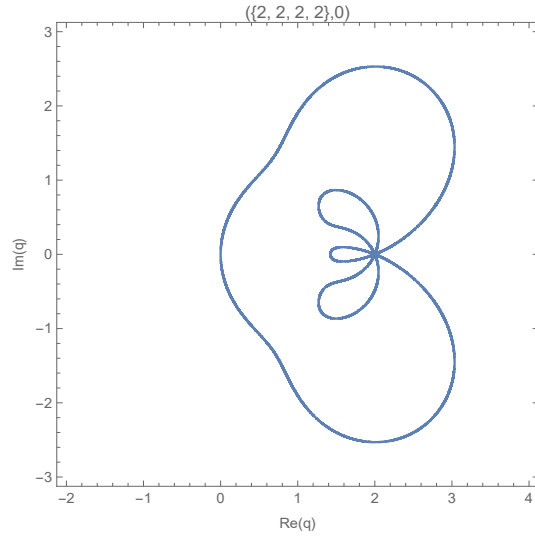


FIG. 10: Locus \mathcal{B} for $r = 4$, $(\{e_1, e_2, e_3, e_4\}, e_g) = (\{2, 2, 2, 2\}, 0)$.

can describe the N_{MP} multiple points as follows. If e_{com} is even, so N_{MP} is odd, then one (and only one) of the MPs is located on the real axis at $q = 2$, while the remaining $N_{MP} = e_{\text{com}} - 2$ MPs are located at the points (7.2) in the complex q plane forming $(e_{\text{com}} - 2)/2$ complex-conjugate pairs. If e_{com} is odd, so N_{MP} is even, then there is no MP on the real axis and the $e_{\text{com}} - 1$ MPs occur at the points (7.3) comprising

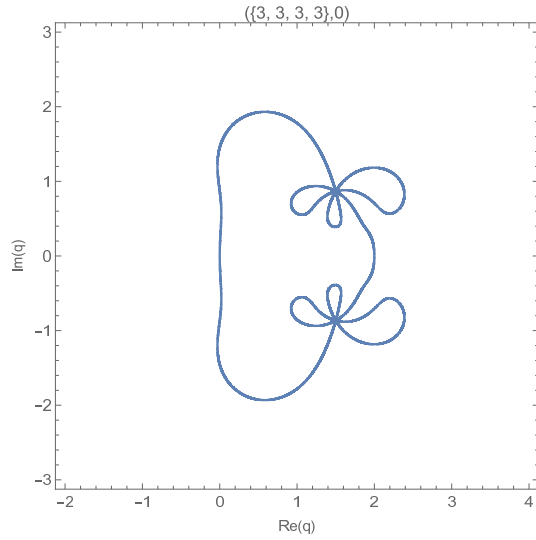


FIG. 11: Locus \mathcal{B} for $r = 4$, $(\{e_1, e_2, e_3, e_4\}, e_g) = (\{3, 3, 3, 3\}, 0)$.

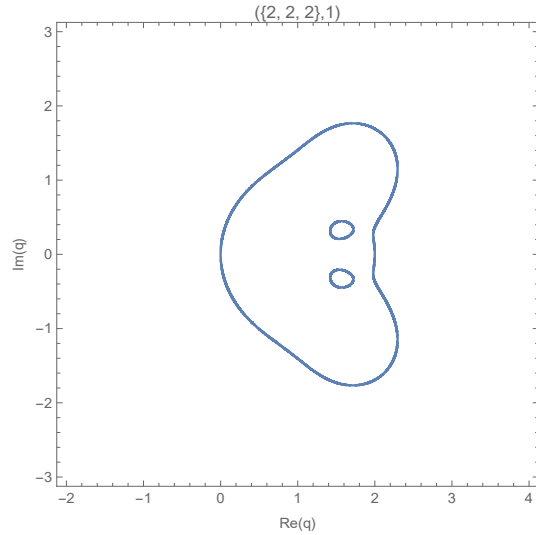


FIG. 12: \mathcal{B} for $r = 3$, $(\{e_1, e_2, e_3\}, e_g) = (\{2, 2, 2\}, 1)$.

$(e_{\text{com}} - 1)/2$ complex-conjugate pairs.

4. At each multiple point, r branches intersect, i.e., there are $2r$ curves emanating out from the MP, with each pair having equal tangents at the MP forming one of these r branches. At each MP, the angle between two adjacent branches on \mathcal{B} is $\phi = \pi/r$.

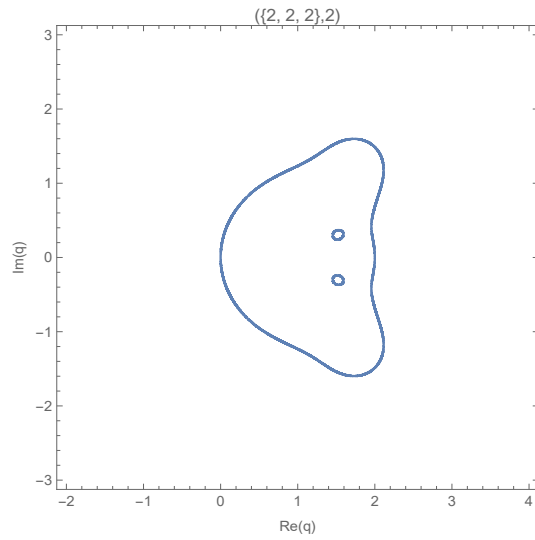


FIG. 13: \mathcal{B} for $r = 3$, $(\{e_1, e_2, e_3\}, e_g) = (\{2, 2, 2\}, 2)$.

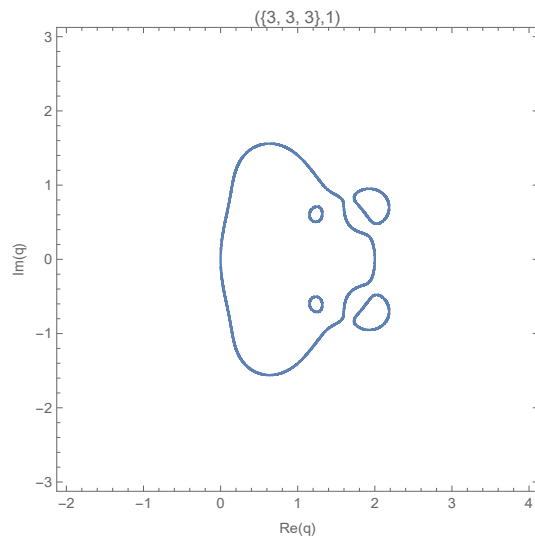


FIG. 14: \mathcal{B} for $r = 3$, $(\{e_1, e_2, e_3\}, e_g) = (\{3, 3, 3\}, 1)$.

5. At each multiple point, two of the $2r$ curves emanating from this MP continue outward to connect to other parts of the outer envelope of \mathcal{B} , while the remaining $2r - 2$ curves form $r - 1$ loops connected (a) to this multiple point or (b) to another multiple point. Examples of case (a) are shown, e.g., in Figs. 2, 4, and 7-11, while examples of case (b) are Figs. 3, 5, and 6. For case (a), especially if there are several loops, the

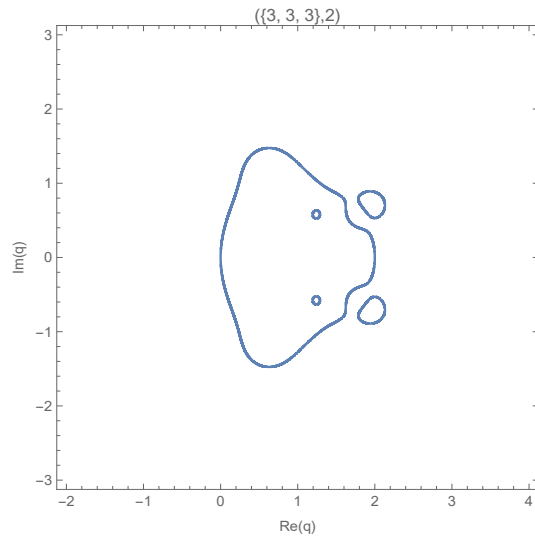


FIG. 15: \mathcal{B} for $r = 3$, $(\{e_1, e_2, e_3\}, e_g) = (\{3, 3, 3\}, 2)$.

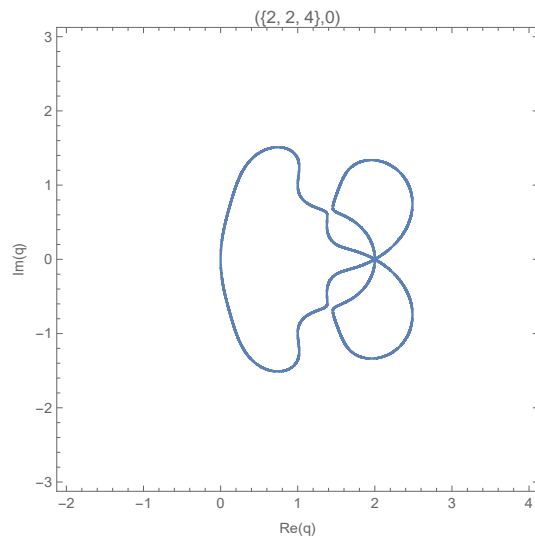


FIG. 16: \mathcal{B} for $r = 3$, $(\{e_1, e_2, e_3\}, e_g) = (\{2, 2, 4\}, 0)$.

corresponding regions can have the appearance of petals of a (generically asymmetric) flower.

6. As a special case of the general property that at each point on \mathcal{B} , $|\lambda_{P,0}| = |\lambda_{P,1}|$, it follows that at each of the points on the real axis where \mathcal{B} crosses this axis, $|\lambda_{P,0}| =$

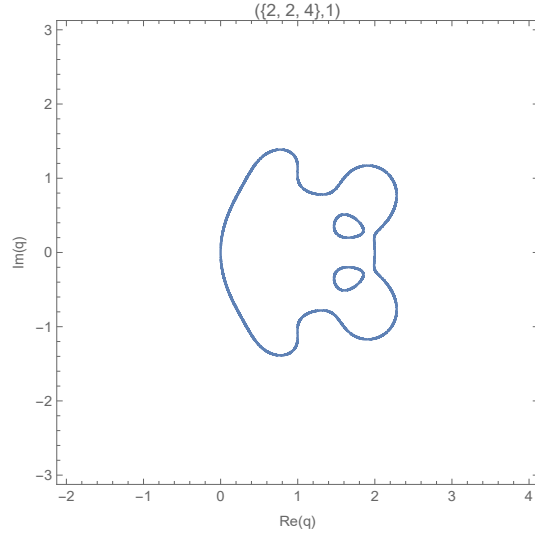


FIG. 17: \mathcal{B} for $r = 3$, $(\{e_1, e_2, e_3\}, e_g) = (\{2, 2, 4\}, 1)$.

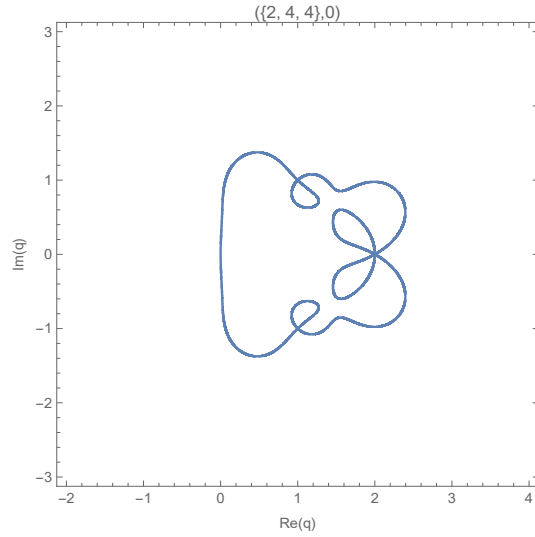


FIG. 18: \mathcal{B} for $r = 3$, $(\{e_1, e_2, e_3\}, e_g) = (\{2, 4, 4\}, 0)$.

$|\lambda_{P,1}|$. When one crosses from a region where $\lambda_{P,0}$ is dominant to a region where $\lambda_{P,1}$ is dominant, there is a non-analytic change in $W(\{G_{\{e\}_r, e_g}\}, q)$. As in the earlier papers (e.g. [20, 23]), the region in the complex plane including the real intervals $q > q_c$ and $q < 0$ is denoted region R_1 , while the interior region including the real interval in the neighborhood of, and to the right of, the origin, is denoted R_2 , and so forth,

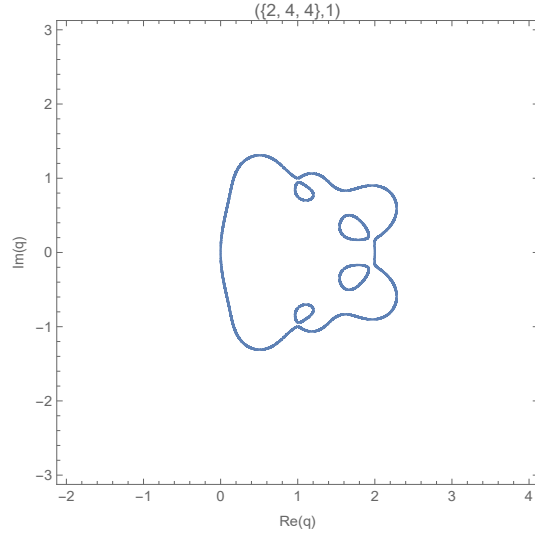


FIG. 19: \mathcal{B} for $r = 3$, $(\{e_1, e_2, e_3\}, e_g) = (\{2, 4, 4\}, 1)$.

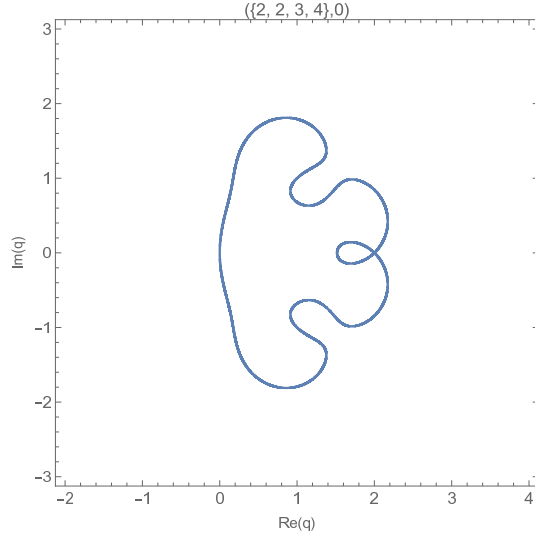


FIG. 20: \mathcal{B} for $r = 4$, $(\{e_1, e_2, e_3, e_4\}, e_g) = (\{2, 2, 3, 4\}, 0)$.

with higher-number subscripts for any other regions, including the notation R_s and R_s^* for complex-conjugate regions. At each point on \mathcal{B} , both $\lambda_{P,0}$ and $\lambda_{P,1}$ have the same magnitude.

7. If e_{com} is even, so N_{MP} is odd, then one of the MPs occurs at $q = 2$. There are then

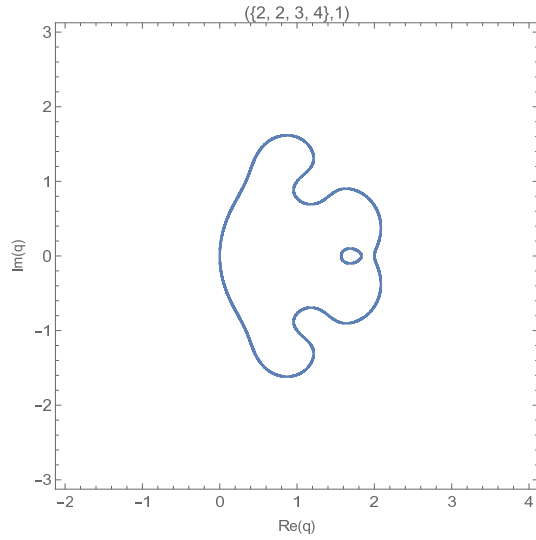


FIG. 21: \mathcal{B} for $r = 4$, $(\{e_1, e_2, e_3, e_4\}, e_g) = (\{2, 2, 3, 4\}, 1)$.

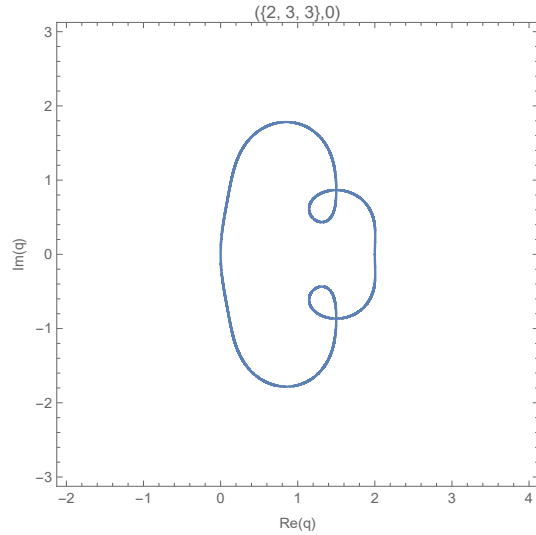


FIG. 22: \mathcal{B} for $r = 3$, $(\{e_1, e_2, e_3\}, e_g) = (\{2, 3, 3\}, 0)$.

two subcases to consider: if (a) r is even, then one of the curves on \mathcal{B} connecting to the MP at $q = 2$ is self-conjugate and crosses the real axis at an interior (int) point denoted q_{int} , while (b) if r is odd, then the $r - 1$ loops form $(r - 1)/2$ complex-conjugate pairs that do not intersect the real axis. Examples of subcase (a) are the loci \mathcal{B} for $e_{\text{com}} = 4, 6, 8$ and $r = 2$ shown in Figs. 2, 4, and 6, and for $e_{\text{com}} = 2$ and $r = 4$ in Fig.

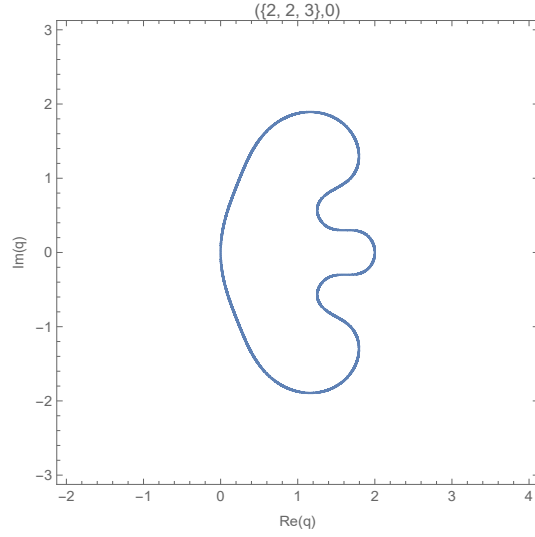


FIG. 23: \mathcal{B} for $r = 3$, $(\{e_1, e_2, e_3\}, e_g) = (\{2, 2, 3\}, 0)$.

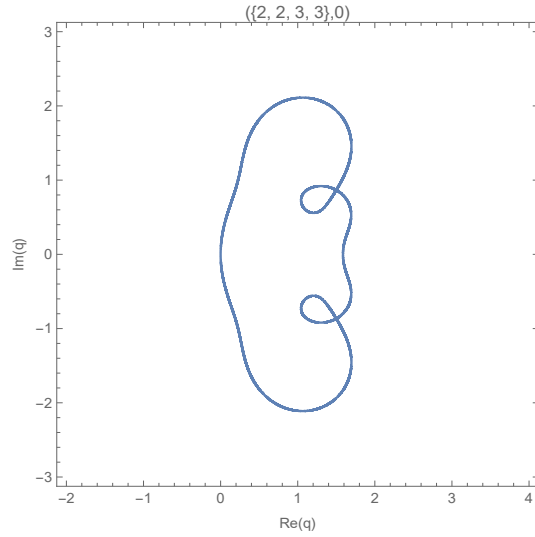


FIG. 24: \mathcal{B} for $r = 4$, $(\{e_1, e_2, e_3, e_4\}, e_g) = (\{2, 2, 3, 3\}, 0)$.

10. Examples of subcase (b) are the loci \mathcal{B} for $e_{\text{com}} = 2, 4$ and $r = 3$ shown in Figs. 7 and 9. We will discuss values of q_{int} further below. In subcase (a), the dominant λ terms on the real axis are as follows: $\lambda_{P,0}$ is dominant if $q > 2$ or $q < 0$ or $q_{\text{int}} < q < 2$, while $\lambda_{P,1}$ is dominant if $0 < q < q_{\text{int}}$. In subcase (b), $\lambda_{P,0}$ is dominant if $q > 2$ or $q < 0$, while $\lambda_{P,1}$ is dominant if $0 < q < 2$.

8. If e_{com} is odd, so N_{MP} is even, then all of these multiple points occur away from the real axis, forming a complex-conjugate set. There are again two subcases to consider, namely: (a') where curves connecting to complex-conjugate MPs on \mathcal{B} cross the real q axis; and (b') where curve(s) connecting to the MPs with $\text{Im}(q) \neq 0$ form loops that do not intersect the real axis. Examples of subcase (a') are the loci \mathcal{B} for $(\{5, 5\}, 0)$ in Fig. 3 and $(\{7, 7\}, 0)$ in Fig. 5, while examples of subcase (b') are the loci \mathcal{B} for $(\{3, 3, 3\}, 0)$ in Fig. 8 and for $(\{3, 3, 3, 3\}, 0)$ in Fig. 11. The situation for subcase (a') is illustrated by loci involving two points at which these curves cross the real axis in the interior of the outer envelope, i.e., with $q < 2$; we denote these two interior crossing points as $q_{\text{int},1}$ and $q_{\text{int},2}$, ordered as $q_{\text{int},1} < q_{\text{int},2}$. For subcase (a'), in addition to the intervals $q > 2$ and $q < 0$, $\lambda_{P,0}$ is also dominant in the real interval $q_{\text{int},1} < q < q_{\text{int},2}$, while $\lambda_{P,1}$ is dominant in the intervals $0 < q < q_{\text{int},1}$ and $q_{\text{int},2} < q < 2$, together with the regions in the complex q plane that can be reached from these respective real intervals without crossing any part of \mathcal{B} . For subcase (b'), $\lambda_{P,0}$ is dominant in the intervals $q > 2$ and $q < 0$, while $\lambda_{P,1}$ is dominant in the interval $0 < q < 2$, together with the regions in the q plane that can be reached from these respective real intervals without crossing \mathcal{B} .
9. For a given r , as e_{com} increases, one observes that parts of \mathcal{B} , especially near to some MPs, exhibit avoided near-crossings with close-by parts of \mathcal{B} . Hence, if one views a diagram with a given locus at low resolution and magnification, there can be apparent intersections, while at higher resolution and magnification, these are seen to be places where the curves nearly intersect, but do not actually do so. These often form approximate barred rings, such that where the bar would intersect the ring at both ends, it only does so at the left hand, while the form of \mathcal{B} on the right side of the ring is an avoided near-crossing. An easily visible example of this is evident in Fig. 2, and this can also be seen, e.g., in Fig. 3, where the avoided near-crossings involve smaller distances between parts of \mathcal{B} . Similar comments on avoided near-crossings having the approximate appearance of barred rings apply to other figures. In Fig. 6 there are four complex-conjugate avoided near-crossings that have the appearance, at low magnification and resolution, of barred rings, together with a complex-conjugate pair of additional avoided near-crossings on the right-hand side of the locus \mathcal{B} that are not of the near-barred ring type. We describe the member of this pair with $\text{Im}(q) > 0$ as follows. Starting from the multiple point at $q = 2$, two curves emanate upward at angles $\pi/4$ and $3\pi/4$. These curves then bend around and approach each other, but do not actually intersect in an avoided near-crossing at $q \simeq 1.9 + 0.4i$, after which they

do cross at a multiple point at $q \simeq 1.8 + 0.7i$.

10. Here, within the EJC class, we describe how the locus \mathcal{B} changes as e_g is increases from 0 to nonzero values. As this increase of e_g is carried out, all of the multiple points that were present for $e_g = 0$ disappear and are replaced by certain sets of “bubble” regions. Thus, in these cases, the locus \mathcal{B} gains new disconnected components. For a given value of e_{com} , each of these bubble regions contract monotonically as e_g increases above 1 and approach points in the limit $e_g \rightarrow \infty$. As with the avoided near-crossings that can occur on \mathcal{B} , if one views plots of \mathcal{B} with small nonzero values of e_g at moderate resolution or magnification, it can be difficult to see the detachment, since the inner part of the boundary of the bubble region is very close to the position of the former multiple point, but the fact that they are separated becomes evident if one uses higher magnification. As e_g increases further, the separation of the bubble regions can easily be seen.
11. For both zero and nonzero e_g , as e_{com} increases beyond 4, the outer envelope of the locus \mathcal{B} approaches (aside from the presence of the $e_{\text{com}} - 1$ multiple points and associated avoided near-crossings) the form of an undular deformation of the unit circle $|q - 1| = 1$ on the upper, lower, and left-hand part of the locus. The angular wavelength interval in the even- e_{com} case is $2\pi/e_{\text{com}}$, while for the odd- e_{com} case, it is $2\pi/(e_{\text{com}} - 1)$.

In Ref. [23], several plots of \mathcal{B} (and associated chromatic zeros) for the $r = 2$ class of cyclic hammock chain graphs were presented. These included several figures for the $r = 2$ EJC class, namely $(\{2, 2\}, e_g)$ and $(\{3, 3\}, e_g)$ with $0 \leq e_g \leq 3$. We note that the locus \mathcal{B} for the family $(\{2, 2\}, 0)$ has a self-conjugate loop extending to the left of $q = 2$ and crossing the real axis at

$$\begin{aligned}
 (\{2, 2\}, 0) : \quad q_{\text{int}} &= \frac{4}{3} + \frac{1}{3}(1 + 3\sqrt{57})^{1/3} - \frac{8}{3}(1 + 3\sqrt{57})^{-1/3} \\
 &= 1.361103,
 \end{aligned} \tag{7.4}$$

This value is listed, together with values of q_{int} for higher even values of e_{com} extending up to 10 in this $r = 2$ EJC class in Table I

We proceed to discuss some features of the loci \mathcal{B} further for various cases $(\{e\}_r, e_g)$. In Figs. 2-6, we show a series of loci \mathcal{B} for the $r = 2$ EJC class with higher values of e_{com} , namely $4 \leq e_{\text{com}} \leq 8$. For plots with $e_g = 0$, since $r = 2$, it follows that $2r = 4$ curves emanate from each multiple point, forming $r = 2$ branches, with angular separation $\phi = \pi/r = \pi/2$ between each curve at a given MP. In Fig. 2 showing \mathcal{B} for the case $(\{4, 4\}, 0)$ there are

TABLE I: Values of q_{int} on \mathcal{B} for members of the $r = 2$, $e_g = 0$ EJC class of cyclic hammock graphs with e_{com} taking even values from 2 to 10.

e_{com}	q_{int}
2	1.361103
4	1.455877
6	1.486632
8	1.496312
10	1.4990415

$e_{\text{com}} = 3$ multiple points, and, in agreement with the general formulas (7.1)-(7.3) from [23], these three MPs are located at $q = 2$ and $q = 1 \pm i$. In this Fig. 2, the MP at $q = 1 - i$ is part of an e -shaped portion of \mathcal{B} involving an avoided near-crossing at the right-hand side of the e , and the complex-conjugate MP at $q = 1 + i$ has the form of a reflection of this about the horizontal axis to produce an inverted e . The MP at $q = 2$ in this Fig. 2 has a loop extending to the left and crossing the real axis at $q = 1.455877$, as listed in Table I. In Fig. 3 showing \mathcal{B} for the case $(\{5, 5\}, 0)$, there are $e_{\text{com}} - 1 = 4$ MPs, comprised of two complex-conjugate pairs. From Eq. (7.3), it follows that these are located at

$$\begin{aligned} \{q_{MP,\ell=1}, q_{MP,\ell=1}^*\} &= 1 + e^{\pm i\pi/5} = \frac{5 + \sqrt{5}}{4} \pm \frac{i\sqrt{2(5 - \sqrt{5})}}{4} \\ &= 1.809017 \pm 0.587785i \end{aligned} \quad (7.5)$$

and

$$\begin{aligned} \{q_{MP,\ell=2}, q_{MP,\ell=2}^*\} &= 1 + e^{\pm 3i\pi/5} \\ &= 0.690983 \pm 0.9587785i \end{aligned} \quad (7.6)$$

The locus \mathcal{B} in this Fig. 3 crosses the real axis at the maximal point $q_c = 2$, and (aside from the ever-present crossing at $q = 0$) at two interior points to the left of q_c , namely

$$(\{5, 5\}, 0) : \quad q_{\text{int},1} = 1.548348, \quad q_{\text{int},2} = 1.860499 \quad (7.7)$$

These values are listed, together with values of $q_{\text{int},1}$ and $q_{\text{int},2}$ for higher odd values of e_{com} extending up to 11 in the $r = 2$, $e_g = 0$ EJC class in Table II. In accordance with our

general discussion above, the term $\lambda_{P,0}$ is dominant on the real intervals $q > 2$, $q < 0$, and $q_{\text{int},1} < q < q_{\text{int},2}$, together with the regions in the complex plane that can be reached from these real intervals without crossing any part of \mathcal{B} . The term $\lambda_{P,1}$ is dominant in the real intervals $0 < q < q_{\text{int},1}$ and $q_{\text{int},2} < q < 2$, together with the regions in the complex plane that can be reached from these real intervals without crossing any part of \mathcal{B} . In addition, $\lambda_{P,0}$ is dominant in the inner part of the “e”-shaped region associated with the multiple point $q_{MP,\ell=1}^*$ and the corresponding region associated inverted “e”-shaped region associated with the MP $q_{MP,\ell=1}$.

TABLE II: Values of $q_{\text{int},1}$ and $q_{\text{int},2}$ on \mathcal{B} for members of the $r = 2$, $e_g = 0$ EJC class of cyclic hammock graphs with e_{com} taking odd values from 3 to 11. The dash for $e_{\text{com}} = 3$ means that there are no interior crossing points on \mathcal{B} in this case.

e_{com}	$q_{\text{int},1}$	$q_{\text{int},2}$
3	—	—
5	1.548348	1.860499
7	1.508787	1.942621
9	1.502023	1.979817
11	1.500493	1.996826

As is evident from these figures and from Table I, in the $r = 2$, $e_g = 0$ EJC class with even e_{com} , as e_{com} increases from 2, the inner crossing point q_{int} increases monotonically, approaching $3/2$ from below as $e_{\text{com}} \rightarrow \infty$. As is also evident from the figures and from Table II, in the $r = 2$, $e_g = 0$ EJC class with odd e_{com} , as e_{com} increases from 3, the smaller interior crossing point $q_{\text{int},1}$ decreases monotonically, approaching $3/2$ from above as $e_{\text{com}} \rightarrow \infty$, while the larger interior crossing point $q_{\text{int},2}$ increases monotonically, approaching the right-most crossing point at $q_c = 2$ from below as $e_{\text{com}} \rightarrow \infty$. Similar analyses of the values of interior crossing points on \mathcal{B} can be carried out for $r \geq 3$.

In Figs. 7-11 we show the respective loci \mathcal{B} for some cyclic hammock graphs in the EJC $e_g = 0$ class with higher rope values $r = 3$ and $r = 4$ in each hammock subgraph. These exhibit the general properties that we have discussed above. Our calculations of \mathcal{B} for higher r generalize the finding in [23] concerning the disappearance of multiple points in loci for families with $e_g = 0$ and their replacement by bubble regions as e_g is increased from zero to nonzero values. We illustrate this with Figs. 12-15. As r increases, more complicated types

of behavior occur as one increases e_g from zero to nonzero values. For example, Fig. 10 showed \mathcal{B} for the $r = 4$ family $(\{2, 2, 2, 2\}, 0)$, which has a multiple point of index 4 at $q = 2$ with three loop regions in the interior, relative to the outer envelope. When one increases e_g from 0 to 1, the locus \mathcal{B} for the family $(\{2, 2, 2, 2\}, 1)$ exhibits a single bubble region in the interior, and for the family $(\{2, 2, 2, 2\}, 2)$, the upper and lower right-hand bulb-like parts of the outer curve on \mathcal{B} have constricted to produce new bubble regions in these areas. Thus, with this family, one observes the appearance of a complex-conjugate pair of bubble regions that did not originate immediately from the disappearance of a multiple point.

We have also calculated loci \mathcal{B} for higher $r \geq 3$ with edge sets $\{e\}_r$ containing some unequal $e_j \in \{e\}_r$. The family $r = 2$ with $(\{e_1, e_2\}, e_g) = (\{2, 4\}, 0)$ was shown in [23] to have a locus \mathcal{B} with a multiple point of index 2 at $q = 2$ that disappears and is replaced by the appearance of a new bubble region for $(\{2, 4\}, e_g)$ with $e_g > 0$, with contraction of the bubble region as e_g is increased through nonzero values. We find a variety of behavior for higher r . For example, Figs. 16 and 17 show the respective loci \mathcal{B} for the $r = 3$ families $(\{2, 2, 4\}, e_g)$ with $e_g = 0$ and $e_g = 1$, respectively. The locus \mathcal{B} for the $(\{2, 2, 4\}, 0)$ family exhibits a multiple point of index 3 at $q = 2$, while for $(\{2, 2, 4\}, 1)$, this MP has disappeared and has been replaced with two bubble regions in the interior of the outer envelope curve. Fig. 18 shows the locus \mathcal{B} for the $r = 3$ family $(\{2, 4, 4\}, 0)$, which exhibits a MP of index 3 at $q = 2$, together with a complex-conjugate pair of MPs of index 2 at $q = 1 \pm i$. When one increases e_g from 0 to 1, these MPs are replaced by four bubble regions, as shown in Fig. 19. Fig. 20 shows \mathcal{B} for the $r = 4$ family $(\{2, 2, 3, 4\}, 0)$, exhibiting a single multiple point of index 2 at $q = 2$. This disappears and is replaced by an interior bubble region when e_g is increased to nonzero values, as shown in Fig. 21 for the family $(\{2, 2, 3, 4\}, 1)$.

We include two other illustrative examples of loci \mathcal{B} for higher r with some unequal e_j edge values in Figs. 22 and 23. Fig. 22 shows \mathcal{B} for the $(\{2, 3, 3\}, 0)$ family, with index-2 multiple points at $q = 1 + e^{\pm\pi i/3}$, which disappear and are replaced by bubble regions for the families $(\{2, 3, 3\}, e_g)$ with $e_g \geq 1$. Fig. 23 depicts \mathcal{B} for the $e_g = 0$ member of the $r = 3$ families $(\{2, 2, 3\}, e_g)$ with a similar property of a smooth locus \mathcal{B} with no multiple points. Both of these families have $q_c = 2$. Ref. [23] also presented results for the $r = 2$ families $(\{2, 3\}, e_g)$ with $0 \leq e_g \leq 3$ for which the respective loci \mathcal{B} have no multiple points and q_c values less than 2. In our discussion above, we have generalized the determination of q_c to $r \geq 3$. As an illustration of a higher- r case with $q_c < 2$, and specifically of the analysis in Eqs. (6.27) and (6.28), we show \mathcal{B} for the $r = 4$ family $(\{2, 2, 3, 3\}, 0)$, which has $q_c < 2$ (and two complex-conjugate) multiple points at $q = 1 + e^{\pm i\pi/3}$.

VIII. ZEROS OF THE POTTS MODEL PARTITION FUNCTION

In the previous section, we have discussed the continuous accumulation loci of the chromatic zeros for the L_m limit of cyclic hammock graphs. In the thermodynamic context, these chromatic zeros are the zeros of the partition function of the $T = 0$ (i.e., $v = -1$) Potts anti-ferromagnet on these cyclic hammock graphs. More generally, it is of interest to investigate the zeros of the partition functions $Z(G_{\{e\}_{r,e_g,m;o}}, q, v)$ and $Z(G_{\{e\}_{r,e_g,m;c}}, q, v)$ in the complex q plane for fixed v and in the complex v plane for fixed q , especially in the L_m limit. Some results on this were given in [24], and we extend these here. Since $Z(G_{\{e\}_{r,e_g,m;o}}, q, v)$ is a polynomial in q and v , one may study the partition function zeros in the q plane for fixed v or the zeros in the v plane for fixed q . As in previous works such as [31], we denote the respective continuous accumulation sets of these zeros in the L_m limit as $\mathcal{B}_q(v)$ and $\mathcal{B}_v(q)$. These are slices through the algebraic variety defined as the continuous accumulation set of the partition function zeros in the $\mathbb{C}^2 \approx \mathbb{R}^4$ space of the variables (q, v) with $q, v \in \mathbb{C}$ in the L_m limit.

Given Eq. (4.1), the zeros of $Z(G_{\{e\}_{r,e_g,m;o}}, q, v)$ in the q plane, besides the one at $q = 0$, are the set of zeros of $\lambda_{Z,0}$, which are discrete (i.e., isolated). The locations of these zeros are independent of m , although each of them has multiplicity m . In contrast, $Z(G_{\{e\}_{r,e_g,m;c}}, q, v)$ has q -plane zeros resulting from cancellations between $(\lambda_{Z,0})^m$ and $(\lambda_{Z,1})^m$. In the L_m limit, almost all of these zeros merge to form the continuous locus $\mathcal{B}_q(v)$. Hence, $\mathcal{B}_q(v)$ for the L_m of cyclic hammock chain graphs is nontrivial (for $v \neq 0$), while $\mathcal{B}_q(v)$ for the L_m limit of open hammock chain graphs is trivial. As with our analysis of chromatic zeros in previous sections, we therefore generally restrict here to considering cyclic hammock chain graphs. For an arbitrary graph G , $Z(G, q, v)$ obeys the property (2.20), that $Z(G, q, v) = q^{n(G)}$ if $v = 0$, so all of the zeros of $Z(G, q, v = 0)$ occur at $q = 0$ (with multiplicity $n(G)$), and $\mathcal{B}_q(v = 0) = \emptyset$. Hence, in the rest of our discussion in this section, unless otherwise specified, we implicitly assume $v \neq 0$, i.e., in the physical context, the temperature is not infinite. Since the loci $\mathcal{B}_q(v)$ and $\mathcal{B}_v(q)$ are formed by zeros of $Z(G_{\{e\}_{r,e_g,m;c}}, q, v)$ in the L_m limit, which, in turn, arise because of the above-mentioned cancellation, one examines the solutions to the equation $|\lambda_{Z,0}| = |\lambda_{Z,1}|$ to study these loci.

The locus $\mathcal{B}_q(v)$ will be of primary interest here, especially since in the limit $v \rightarrow -1$, this becomes the continuous accumulation set of chromatic zeros. The other locus, \mathcal{B}_v (the accumulation set of Fisher zeros) is of somewhat less interest, since the L_m limit of these hammock chain graphs is essentially one-dimensional, and hence, for physical values of q , the corresponding Potts model with either sign of J does not exhibit a phase transition at any nonzero temperature.

We first recall some elementary properties of $\mathcal{B}_q(v)$, generalizing our discussion above of $\mathcal{B}(v)$ for $v = -1$. As is evident from Eq. (2.18), for an arbitrary graph G , if $v \in \mathbb{R}$, then $Z(G, q, v)$ is a polynomial in q with real coefficients and hence, for a given v , the action of complex conjugation, $q \rightarrow q^*$, induces an automorphism of the resultant set of zeros of $Z(G, q, v)$ in the complex q plane. Given that v is in the real ranges listed above for the physical Potts antiferromagnet or ferromagnet, it follows in the specific context of the L_m limit of hammock chain graphs that $\mathcal{B}_q(v)$ maps into itself under the complex conjugation $q \rightarrow q^*$. Similarly, if $q \in \mathbb{R}$, then $Z(G, q, v)$ is a polynomial in v with real coefficients and hence, for a fixed physical (and hence real, nonnegative) q , the action of complex conjugation, $v \rightarrow v^*$, induces an automorphism of the set of zeros of $Z(G, q, v)$ in the complex v plane. Again, it follows that for a fixed physical value of q , the continuous accumulation locus $\mathcal{B}_v(q)$ is invariant under the complex conjugation $v \rightarrow v^*$. For general antiferromagnetic v , the maximal point at which $\mathcal{B}_q(v)$ crosses the real- q axis is denoted $q_c = q_c(v)$. Since we focus on $\mathcal{B}_q(v)$ rather than $\mathcal{B}_v(q)$ below, unless otherwise indicated, we use the simplified notation $\mathcal{B}_q(v) = \mathcal{B}_q$.

In Figs. 25 and 26 we show \mathcal{B}_q for illustrative finite-temperature values of v , namely $v = -0.5$, for the Potts antiferromagnet and $v = 1$ for the Potts ferromagnet. Comparing the locus in Fig. 25 with the zero-temperature (i.e., $v = -1$) locus in Fig. 7, one sees that \mathcal{B}_q contracts both vertically and horizontally, while continuing to pass through $q = 0$. This contraction is a general feature observed before for other families of graphs (e.g. [31, 45]) and continues as $v \rightarrow 0^-$, ending as \mathcal{B} degenerates to a point at $q = 0$ for $v = 0$, in accordance with Eq. (2.20). The locus \mathcal{B}_q in Fig. 26 for the illustrative finite-temperature ferromagnetic value $v = 1$ exhibits the feature that \mathcal{B} does not cross the positive- q axis, and this is a general property for the ferromagnetic range $v \geq 0$.

There are several properties of \mathcal{B}_q for the cyclic hammock chain graphs that hold for general physical v . These include the following [24] : (i) \mathcal{B} is compact; (ii) \mathcal{B} passes through the point $q = 0$; and (iii) \mathcal{B} encloses regions in the complex q plane. These are the generalizations of properties (B1)-(B3) proved in [23] for $r = 2$ and the special case $v = -1$ and are proved in a similar manner for general v . As is clear from our discussion of \mathcal{B}_q for the zero-temperature antiferromagnetic value $v = -1$, the extension to the analysis of $\mathcal{B}(v)$ for general finite-temperature antiferromagnetic and ferromagnetic values of v has an interesting wealth of properties. Further analysis of these properties of $\mathcal{B}_q(v)$ will be given in a sequel article.

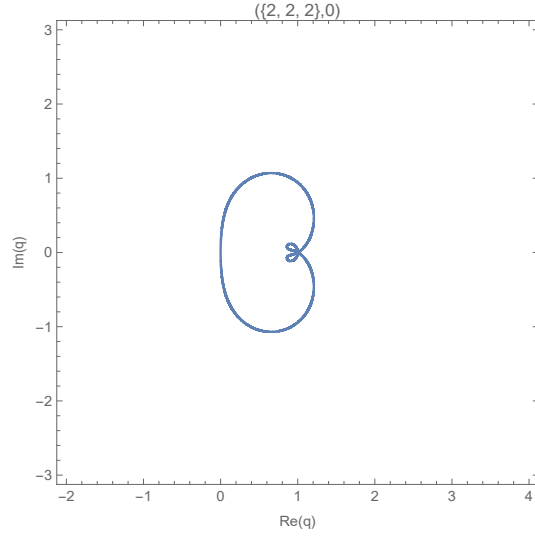


FIG. 25: \mathcal{B} for $\{G_{\{e\}_{r=3, e_g; c}}\}$ with $(\{e_1, e_2, e_3\}, e_g) = (2, 2, 2), 0$ and $v = -0.5$.

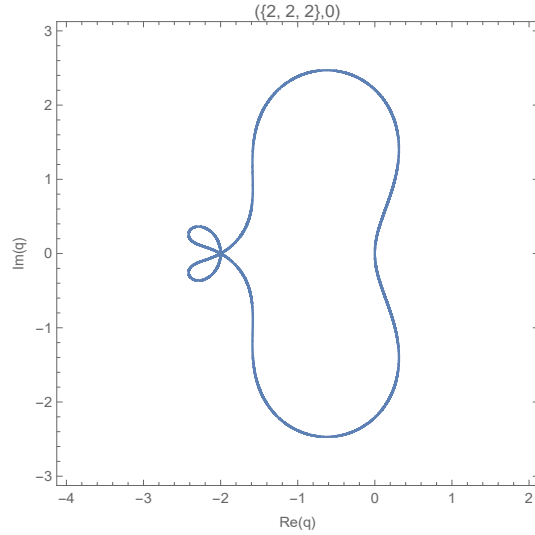


FIG. 26: \mathcal{B} for $\{G_{\{e\}_{r=3, e_g; c}}\}$ with $(\{e_1, e_2, e_3\}, e_g) = (\{2, 2, 2\}, 0)$ and $v = 1$.

IX. FREE ENERGY

In the context of statistical physics, it is of interest to calculate the Gibbs free energy per vertex, \mathcal{G} , of the q -state Potts model on these hammock chain graphs. It is convenient to define a reduced, dimensionless free energy f according to $\mathcal{G} = -k_B T f$, where, as above,

T is the temperature. We take the limit $m \rightarrow \infty$ in evaluating f and recall the notation $\{G_{\{e\}_{r,e_g,BC}}\}$.

For a strip (chain) graph G and a set of special values of q , denoted $\{q_x\}$, one can encounter the noncommutativity [31]

$$\lim_{q \rightarrow q_x} \lim_{n(G) \rightarrow \infty} Z(G, q, v)^{1/n} \neq \lim_{n(G) \rightarrow \infty} \lim_{q \rightarrow q_x} Z(G, q, v)^{1/n}. \quad (9.1)$$

The corresponding noncommutativity of limits in the case of $P(G, q)$ had also been noted in [20]. For the graphs of interest here, the set $\{q_x\}$ includes $\{0, 1\}$. When studying the $m \rightarrow \infty$ limit of $[Z(G_{\{e\}_{r,e_g,m,BC}}, q, v)]^{1/n}$ here, we choose the first order of limits, i.e., we take the limit $n \rightarrow \infty$ first and then the limit $q \rightarrow q_x$. It should also be recalled that if $J > 0$ (so $v \geq 0$), then the cluster representation (2.18) defines a Gibbs measure for nonnegative real, as well as nonnegative integral q , as is clear since each term $q^{k(G')} v^{e(G')}$ in (2.18) is nonnegative. This is also true in the antiferromagnetic case $J < 0$ if q is a positive integer, since one can revert back to the Hamiltonian form $Z(G, q, v) = \exp[K \sum_{e_{ij}} \delta_{\sigma_i \sigma_j}]$, which is positive-definite. However, if $J < 0$, then for positive but nonintegral q , the cluster representation (2.18) can yield a negative value for $Z(G, q, v)$ and hence not satisfy the condition for a Gibbs measure. We will consider the limit of an infinite-length chain graph, i.e., $m \rightarrow \infty$ for the calculation of the free energy per vertex. As a quasi-one-dimensional system, this corresponds to a physical 1D thermodynamic limit. In this limit, with physical values of input parameters, the dimensionless free energy per vertex for the Potts model, denoted f , is

$$\begin{aligned} f(\{G_{\{e\}_{r,e_g}}\}, q, v) &= \lim_{m \rightarrow \infty} \frac{1}{n} \ln [Z(G_{\{e\}_{r,e_g,m,BC}})] \\ &= \frac{1}{[(\sum_{j=1}^r e_j) + e_g - (r - 1)]} \ln(\lambda_{Z,0}), \end{aligned} \quad (9.2)$$

where $\lambda_{Z,0}$ was given in Eq. (4.3). In Eq. (9.2) we have dropped the subscript BC in $\{G_{\{e\}_{r,e_g,BC}}\}$ since f is independent of boundary conditions here, as is a necessary condition of the thermodynamic limit. We recall that the independence of boundary conditions implies that the dominant term among $(\lambda_{Z,0})^m$ and $(\lambda_{Z,1})^m$, must be $(\lambda_{Z,0})^m$, since this is the only term that contributes to both $Z(G_{\{e\}_{r,e_g,m,o}}, q, v)$ and to $Z(G_{\{e\}_{r,e_g,m,c}}, q, v)$.

From the dimensionless free energy per vertex, $f(\{G_{\{e\}_{r,e_g}}\}, q, v)$, one can then calculate the internal energy U and specific heat C per vertex. Since the expressions are somewhat lengthy, we do not include them here. A salient difference between the hammock graphs for $r = 2$ and for $r \geq 3$ is that in the $r = 2$ case, as is evident from Eq. (4.9), the dependence of $\lambda_{Z,0;r=2}$, and hence also the dimensionless free energy f , on the edges e_1 and e_2 in the

set $\{e\}_{r=2}$ is only through their sum, $p = e_1 + e_2$, the number of sides of each polygon in the chain. As is clear from Eq. (4.3), for hammock graphs with $r \geq 3$, this simplification no longer holds, i.e., the dependence of $\lambda_{Z,0;r \geq 3}$ on the r edges $e_j \in \{e\}_r$ is not expressible simply as a function of their sum.

X. FLOW POLYNOMIALS

Another important one-variable special case of the Tutte polynomial is the flow polynomial of a graph G , denoted $F(G, q)$ [53]. To define this polynomial, one considers a connected graph and chooses an orientation for each edge. Next, one assigns an element of a finite abelian group \mathbb{Z}_q as a discretized flow along a given oriented edge and imposes two conditions: (i) there is flow conservation mod q at each vertex, i.e., no sources or sinks, and (ii) the flow along each edge must be nonzero, since a zero flow on an edge would be equivalent to the absence of this edge in the graph. This defines a nowhere-zero flow on the graph. Henceforth, for brevity we will refer to nowhere-zero flows on a graph simply as flows on the graph. Just as in solving Kirchhoff's equations in electrical circuit theory, the enumeration of these flows is independent of the convention that one takes for the orientation of each edge [17]. The flow polynomial thus depends only on the structure of the graph G itself and is given in terms of the Tutte polynomial by the relation

$$F(G, q) = (-1)^{c(G)} T(G, x = 0, y = 1 - q) , \quad (10.1)$$

where, as above, $c(G)$ denotes the number of linearly independent circuits on G . The minimum (integer) number q such that a graph G has a (nowhere-zero) q -flow is denoted $\phi(G)$. If a (connected) graph G contains any bridge, then the flow polynomial vanishes identically. The open hammock chain graph $G_{\{e\}_r, e_g, m; o}$ contains at least one bridge if (i) $e_g \geq 1$ or (ii) $r = 1$ and $e_1 \geq 1$. Hence,

$$F(G_{\{e\}_r, e_g, m; o}, q) = 0 \quad \text{if } e_g \geq 1 \quad (10.2)$$

and

$$F(G_{\{e\}_r, e_g, m; o}, q) = 0 \quad \text{if } r = 1 \text{ and } e_1 \geq 1 \quad (10.3)$$

From our general results for $T(G_{\{e\}_r, e_g, m, BC}, x, y)$, we calculate the flow polynomials

$$F(G_{\{e\}_r, e_g, m; o}, q) = \delta_{e_g, 0} [(q - 1)D_r]^m \quad (10.4)$$

and

$$F(G_{\{e\}_r, e_g, m; c}, q) = \delta_{e_g, 0} [(q - 1)D_r]^m + (q - 1)[D_{r+1}]^m , \quad (10.5)$$

where δ_{ij} is the Kronecker delta function. For $r = 2$, these general- r results agree with Eqs. (8.3) and (8.4)) in [24]. A notable property of these results is that $F(G_{\{e\}_{r,e_g,m;o}, q})$ and $F(G_{\{e\}_{r,e_g,m;c}, q})$ depend on r , but are independent of the values of the edges $e_j \in \{e\}_r$. This property is easily understandable, since if a given flow is allowed, it does not depend on how many edges there are in any of the ‘‘ropes’’ making up a given hammock subgraph.

We comment on some properties of our general results (10.4) and (10.5), beginning with the open hammock chain graphs. Let us assume that $e_g = 0$ and $r \geq 2$ so that there are no bridges in $G_{\{e\}_{r,e_g,m;o}}$. From Eq. (10.4) we see that (i) $G_{\{e\}_{r,e_g=0,m;o}}$ has a 2-flow (i.e., $F(G_{\{e\}_{r,e_g=0,m;o}, q = 2}) > 0$) only if r is even; (ii) there is precisely one 2-flow on $G_{\{e\}_{r,e_g=0,m;o}}$ if r is even, i.e., $F(G_{\{e\}_{r,e_g=0,m;o}, q = 2}) = 1$ for even r ; and (iii) for even r , $\phi(G_{\{e\}_{r,e_g=0,m;o}}) = 2$. We proceed to prove these properties. Since D_r vanishes at $q = 2$ if r is odd, it follows that $F(G_{\{e\}_{r,e_g,m;o}, q}) = 0$ at $q = 2$ if r is odd. If $q = 2$, i.e., the abelian group used for the flows is \mathbb{Z}_2 , then $1 = -1 \pmod{2}$. Now (with $e_g = 0$ so flows are possible on this open hammock chain graph) if $q = 2$, then there is only one nonzero current of flow on a given oriented edge \vec{e}_j , namely a flow of 1 unit in the direction of the arrow. If and only if r is even, then the unit flows on $r/2$ ropes entering the end vertex of each hammock subgraph on the open chain can flow out again as unit flows on the orthogonal set of $r/2$ ropes, but this is not possible if r is odd. Equivalently, we can regard this flow as unit flows on all r ropes going into the end vertex and use the fact that $r \times 1 = 0 \pmod{2}$ if and only if r is even. This proves property (i). Clearly, there is only one such flow configuration, which proves (ii). The existence of this flow proves property (iii).

For sufficiently large fixed value of q , $F(G_{\{e\}_{r,e_g=0,m;o}, q})$ is a monotonically increasing function of r . This is a consequence of the property that D_r is a polynomial of degree $r - 2$, going like q^{r-2} for large q . If r is odd, then there is a small interval of q extending from $q = 2$ to a slightly larger value of q for which, if r is odd and s is even, then $D_r < D_s$ even though $r > s$, reflecting the zero at $q = 2$ in D_r for odd s . For example, let us compare $D_4 = q^2 - 3q + 3$ and $D_5 = (q - 2)(q^2 - 2q + q)$ in the real- q interval slightly above $q = 2$. In the interval $2 \leq q \leq 2.54369$ (where the upper end of this interval is determined as the unique real root of the cubic equation $q^3 - 5q^2 + 9q - 7 = 0$), $D_4 > D_5$. However, for all $q > 2.54369$, $D_5 > D_4$. Similarly, $D_7 < D_6$ for $2 \leq q \leq 2.38809$, but $D_7 > D_6$ for $q > 2.38809$. Hence, if one restricts q to integral values $q \geq 3$, then $F(G_{\{e\}_{r,e_g=0,m;o}, q})$ is a monotonically increasing function of r .

We also remark on properties of $F(G_{\{e\}_{r,e_g=0,m;c}, q})$ for the cyclic hammock chain graphs. Both for $e_g = 0$ and for $e_g \geq 1$, the cyclic hammock chain graph allows more q -flows than the open hammock graph. This is a consequence of the possibility that q -flows on the cyclic graph can make a global circuit around the chain. In particular, even if $e_g > 0$, so there are

no q -flows on the open hammock graph, there are still q -flows on the cyclic hammock graph provided that the second term in Eq. (10.5) is nonzero, which is the case if r is odd or if r is even and $q \geq 3$. As with the open hammock chain, for a sufficiently large fixed value of q , $F(G_{\{e\}_{r,e_g,m;c}}(q))$ is a monotonically increasing function of r .

For fixed m , as $q \rightarrow \infty$, the flow polynomials behave asymptotically as

$$F(G_{\{e\}_{r,e_g,m;o}}(q)) \sim \delta_{e_g,0} q^{m(r-1)} \quad \text{as } q \rightarrow \infty \quad (10.6)$$

and

$$F(G_{\{e\}_{r,e_g,m;c}}(q)) \sim \delta_{e_g,0} q^{m(r-1)} + q^{m(r-1)+1} \quad \text{as } q \rightarrow \infty . \quad (10.7)$$

Another comparison is with flow polynomials for strip graphs of various lattice types. It is natural to consider the simplest strip graph for this comparison, namely a one-dimensional line graph of length n vertices. If this has open boundary conditions, there are no q -flows, so we restrict to the case of cyclic boundary conditions, for which one has the elementary result $F(C_n, q) = q - 1$. We compare this with $F(G_{\{e\}_{r,e_g,m;c}}(q))$. If $r = 1$, then the cyclic hammock graph reduces to a circuit graph C_n with $n = m(e_1 + e_g)$ vertices, and hence the same flow polynomial, namely $q - 1$. For most choices of r , e_g , q , and m , there are more q -flows (typically exponentially more) on a cyclic hammock graph with m hammock subgraphs than on C_n . For example, if $r = 3$, $e_g = 0$, and $q = 3$, then $F(G_{\{e\}_{3,e_g=0,m;c}}(q = 3)) = 2^m + 2 \cdot 3^m$, while if $r = 3$, $e_g = 1$, and $q = 3$, then $F(G_{\{e\}_{3,e_g=1,m;c}}(q = 3)) = 2 \cdot 3^m$, as contrasted with $F(C_n, q = 3) = 2$. However, in certain cases, there may be an equal number of q -flows on cyclic hammock graphs and the circuit graph, or even no q -flows on cyclic hammock graphs and a nonzero number of q -flows on a circuit graph. For example, if $r \geq 2$ and $e_g = 0$, then, from Eq. (10.5) we have $F(G_{\{e\}_{r,e_g=0,m;c}}(q)) = [(q - 1)D_r]^m + (q - 1)[D_{r+1}]^m$. Continuing to hold $e_g = 0$, if also $q = 2$ and r is even, then, because $D_{\text{odd}} = 0$ at $q = 2$, the second term vanishes, and $D_{r \text{ even}} = 1$ at $q = 2$, so $F(G_{\{e\}_{r \text{ even},e_g=0,m;c}}(q = 2)) = 1$, the same as for the circuit graph with $q = 2$. If $e_g > 1$, then $F(G_{\{e\}_{r,e_g,m;c}}(q)) = (q - 1)[D_{r+1}]^m$, so if also r is even and $q = 2$, then $F(G_{\{e\}_{r \text{ even},e_g,m;c}}(q = 2)) = 0$, and hence there are no 2-flows on these cyclic hammock graphs, whereas in contrast, there is one 2-flow on C_n . Finally, we observe that the zeros of flow polynomials and reliability polynomials are of interest but are beyond the scope of the current work; an analysis of these will be given elsewhere.

XI. RELIABILITY POLYNOMIALS

A communication network, such as the internet, can be represented by a graph, with the vertices of the graph representing the nodes of the network and the edges of the graph

representing the communication links between these nodes. In analyzing the reliability of a network, one is interested in the probability that there is a working communications route between any node and any other node [55, 56]. This quantity is the (all-terminal) reliability function. This is often studied using a simplification in which one assumes that each node is operating with probability p_{node} and each link (bond, abbreviated b) is operating with probability p_b . As probabilities, p_{node} and p_b lie in the interval $[0,1]$. The dependence of the all-terminal reliability function $R_{tot}(G, p_{node}, p_b)$ on p_{node} is an overall factor of $(p_{node})^n$; i.e., $R_{tot}(G, p_{node}, p_b) = (p_{node})^n R(G, p_b)$. The difficult part of the calculation of $R_{tot}(G, p_{node}, p_b)$ is thus the part that depends on the bonds, $R(G, p_b)$. The function $R(G, p_b)$ is given by

$$R(G, p_b) = \sum_{\tilde{G} \subseteq G} p_b^{e(\tilde{G})} (1 - p_b)^{e(G) - e(\tilde{G})} \quad (11.1)$$

where \tilde{G} is a connected spanning subgraph of G . Each term in this sum is the probability that the communication links $\tilde{E} \in \tilde{G}$ are functioning (equal to $p_b^{e(\tilde{G})}$) times the probability that the other links, $E - \tilde{E}$, are not functioning (equal to $(1 - p_b)^{e(G) - e(\tilde{G})}$). Since $e(\tilde{G})$ and $e(G) - e(\tilde{G})$ are both nonnegative, Eq. (11.1) shows that $R(G, p_b)$ is a polynomial in p_b . From its definition, $R(G, p_b)$ is clearly a monotonically increasing function of $p_b \in [0, 1]$ with the boundary values $R(G, 0) = 0$ and $R(G, 1) = 1$. $R(G, p_b)$ is given in terms of the Tutte polynomial, evaluated with $x = 1$ (guaranteeing that \tilde{G} is a connected spanning subgraph of G) and $y = y_b$, where

$$y_b = \frac{1}{1 - p_b} \quad i.e., \quad v_b = y_b - 1 = \frac{p_b}{1 - p_b}, \quad (11.2)$$

by the relation

$$R(G, p_b) = p_b^{n(G) - 1} (1 - p_b)^{e(G) + 1 - n(G)} T(G, 1, \frac{1}{1 - p_b}). \quad (11.3)$$

From our calculation of the general Tutte polynomials for $G_{\{e\}_{r, e_g, m; o}}$ and $G_{\{e\}_{r, e_g, m; c}}$ using the relation Eq. (11.3), we can compute the corresponding reliability polynomials $R(G_{\{e\}_{r, e_g, m; o}}, p_b)$ and $R(G_{\{e\}_{r, e_g, m; c}}, p_b)$. For this purpose, it is helpful to use Eqs. (3.18) and (3.19). For the open hammock chain graphs we obtain

$$R(G_{\{e\}_{r, e_g, m; o}}, p_b) = [(p_b^{(\sum_{j=1}^r e_j) + e_g - r} \mu_{R,0})]^m, \quad (11.4)$$

where

$$\mu_{R,0} = \prod_{j=1}^r \left\{ (1 - p_b) e_j + p_b \right\} - (1 - p_b)^r \prod_{j=1}^r e_j. \quad (11.5)$$

The quantity $\mu_{R,0}$ always has a factor of p_b , so for general r , $R(G_{\{e\}_{r,e_g,m;o},p_b})$ has an overall factor of $(p_b)^{m[(\sum_{j=1}^r e_j)+e_g-(r-1)]}$. For example, if $r = 2$, then

$$R(G_{\{e\}_{r=2,e_g,m;o},p_b}) = \left[p_b^{e_1+e_2+e_g-1} [(e_1 + e_2)(1 - p_b) + p_b] \right]^m \quad (11.6)$$

and if $r = 3$, then

$$\begin{aligned} R(G_{\{e\}_{r=3,e_g,m;o},p_b}) &= \left[p_b^{(\sum_{j=1}^3 e_j)+e_g-2} \times \right. \\ &\times \left. \left\{ (e_1 e_2 + e_1 e_3 + e_2 e_3)(1 - p_b)^2 + (e_1 + e_2 + e_3)p_b(1 - p_b) + p_b^2 \right\} \right]^m. \end{aligned} \quad (11.7)$$

For the cyclic hammock chain graphs, we find the general formula

$$\begin{aligned} R(G_{\{e\}_{r,e_g,m;c},p_b}) &= p_b^{m[(\sum_{j=1}^r e_j)+e_g-r]} (\mu_{R,0})^{m-1} \times \\ &\times \left[p_b^{-1} [m e_g(1 - p_b) + p_b] \mu_{R,0} + m(1 - p_b)^r \prod_{j=1}^r e_j \right]. \end{aligned} \quad (11.8)$$

In the cases where $r = 2$ and $r = 3$, Eq. (11.8) yields the following:

$$\begin{aligned} R(G_{\{e\}_{r=2,e_g,m;c},p_b}) &= p_b^{m(e_1+e_2+e_g-1)-1} \left[(e_1 + e_2)(1 - p_b) + p_b \right]^{m-1} \times \\ &\times \left[\left\{ m e_g(1 - p_b) + p_b \right\} \left\{ (e_1 + e_2)(1 - p_b) + p_b \right\} + m e_1 e_2 (1 - p_b)^2 \right]. \end{aligned} \quad (11.9)$$

and

$$\begin{aligned} R(G_{\{e\}_{r=3,e_g,m;c},p_b}) &= p_b^{m[(\sum_{j=1}^3 e_j)+e_g-2]-1} \times \\ &\times \left[(e_1 e_2 + e_1 e_3 + e_2 e_3)(1 - p_b)^2 + (e_1 + e_2 + e_3)p_b(1 - p_b) + p_b^2 \right]^{m-1} \times \\ &\times \left[\left(m e_g(1 - p_b) + p_b \right) \left\{ (e_1 e_2 + e_1 e_3 + e_2 e_3)(1 - p_b)^2 + (e_1 + e_2 + e_3)p_b(1 - p_b) + p_b^2 \right\} \right. \\ &\left. + m e_1 e_2 e_3 (1 - p_b)^3 \right] \end{aligned} \quad (11.10)$$

XII. PERCOLATION CLUSTERS

In this section we use our results to calculate a quantity of interest in the area of bond percolation. We first briefly mention some necessary background (reviews include [58, 59]).

Consider a connected graph G and assume that the vertices are definitely present, but each edge (bond, b) is present only with a probability $p_b \in [0, 1]$. In the usual statistical mechanical context, one usually considers a limit in which the number of vertices $n \rightarrow \infty$. An important quantity is the average number of connected components (= clusters) in G . For a given G , we denote this average cluster number per vertex as $\langle k \rangle_G$. This is given by

$$\begin{aligned} \langle k \rangle_G &= \frac{(1/n) \sum_{G'} k(G') p_b^{e(G')} (1 - p_b)^{e(G) - e(G')}}{\sum_{G'} p_b^{e(G')} (1 - p_b)^{e(G) - e(G')}} \\ &= \frac{(1/n) \sum_{G'} k(G') v_b^{e(G')}}{\sum_{G'} v_b^{e(G')}} , \end{aligned} \quad (12.1)$$

where G' is a spanning subgraph of G , as above, and v_b was defined in Eq. (11.2). Hence, in the $n \rightarrow \infty$ limit, the average cluster number per vertex, $\langle k \rangle_{\{G\}}$, is given by

$$\langle k \rangle_{\{G\}} = \left. \frac{\partial f(\{G\}, q, v)}{\partial q} \right|_{q=1, v=v_b} . \quad (12.2)$$

This is independent of the longitudinal boundary conditions on the chain. Two general properties holding for an arbitrary graph G may be noted. First, if $p_b = 1$, then there is just one cluster, consisting of the entire graph, and hence the division by n yields 0, so

$$\langle k \rangle_G = 0 \quad \text{if } p_b = 1 . \quad (12.3)$$

This implies that $\langle k \rangle_G$ contains at least one factor of $(1 - p_b)$. Second, if $p_b = 0$, then there are n clusters each consisting of one of the n vertices of G , so

$$\langle k \rangle_G = 1 \quad \text{if } p_b = 0 . \quad (12.4)$$

For a given G , $\langle k \rangle_G$ is a monotonically decreasing function of p_b , decreasing from $\langle k \rangle_G = 1$ at $p_b = 0$ to $\langle k \rangle_G = 0$ at $p_b = 1$.

For the hammock chain graphs under consideration here, the average cluster number $\langle k \rangle_{\{G_{\{e\}r, eg}\}}$ is determined by substituting Eq. (9.2) in Eq. (12.2). We calculate

$$\begin{aligned} \langle k \rangle_{\{G_{\{e\}r, eg}\}} &= \frac{1}{(\sum_{j=1}^r e_j) + e_g - (r - 1)} \times \\ &\times \left[-r + e_g(1 - p_b) + \sum_{j=1}^r \left\{ e_j(1 - p_b) + p_b^{e_j} \right\} + \prod_{j=1}^r (1 - p_b^{e_j}) \right] \end{aligned} \quad (12.5)$$

For $r = 2$, Eq. (12.5) reduces to the expression given as Eq. (10.3) in [24], which reads, in our current notation, as

$$\begin{aligned}\langle k \rangle_{\{G_{\{e\}}_{r=2, e_g}\}} &= \frac{1}{(e_1 + e_2 + e_g - 1)} \left[-1 + (e_1 + e_2 + e_g)(1 - p_b) + p_b^{e_1+e_2} \right] \\ &= \left(\frac{1 - p_b}{e_1 + e_2 + e_g - 1} \right) \left[e_1 + e_2 + e_g - \left(\sum_{j=0}^{e_1+e_2-1} p_b^j \right) \right].\end{aligned}\quad (12.6)$$

The expression in the second line of Eq. (12.6) explicitly shows the factor of $(1 - p_b)$ in $\langle k \rangle_{\{G_{\{e\}}_{r=2, e_g}\}}$. As an illustration of a result for higher r , if $r = 3$, then the general result (12.5) yields

$$\begin{aligned}\langle k \rangle_{\{G_{\{e\}}_{r=3, e_g}\}} &= \frac{1}{((\sum_{j=1}^3 e_j) + e_g - 2)} \left[-2 + \left\{ (\sum_{j=1}^3 e_j) + e_g \right\} (1 - p_b) \right. \\ &\quad \left. + \left\{ p_b^{e_1+e_2} + p_b^{e_1+e_3} + p_b^{e_2+e_3} \right\} - p_b^{e_1+e_2+e_3} \right].\end{aligned}\quad (12.7)$$

Again, one can reexpress this with an explicit overall factor of $(1 - p_b)$ by using the identity $p_b^t - 1 = (p_b - 1) \sum_{i=0}^{t-1} p_b^i$:

$$\begin{aligned}\langle k \rangle_{\{G_{\{e\}}_{r=3, e_g}\}} &= \left(\frac{1 - p_b}{(\sum_{j=1}^3 e_j) + e_g - 2} \right) \left[\left\{ (\sum_{j=1}^3 e_j) + e_g \right\} \right. \\ &\quad \left. - \left\{ \sum_{i=0}^{e_1+e_2-1} p_b^i + \sum_{i=0}^{e_1+e_3-1} p_b^i + \sum_{i=0}^{e_2+e_3-1} p_b^i \right\} + \sum_{i=0}^{e_1+e_2+e_3-1} p_b^i \right].\end{aligned}\quad (12.8)$$

Expressions for $\langle k \rangle_{\{G_{\{e\}}_{r, e_g}\}}$ for the $m \rightarrow \infty$ limits of higher- r hammock chain graphs can be calculated from our general formula (12.5) in a similar manner.

XIII. SOME GRAPHICAL QUANTITIES

A. General

Special valuations of the Tutte polynomial of a graph for particular x and y yield enumerations of various types of subgraphs of the given graph. Recall that a tree graph is a connected graph with no circuits. A spanning tree of a graph G is a spanning subgraph of G that is also a tree. A spanning forest of a graph G is a spanning subgraph

of G that may consist of more than one connected component but contains no circuits. The special valuations of interest include (i) $T(G, 1, 1) = N_{ST}(G)$, the number of spanning trees (ST) of G ; (ii) $T(G, 2, 1) = N_{SF}(G)$ the number of spanning forests (SF) of G ; (iii) $T(G, 1, 2) = N_{CSSG}(G)$, the number of connected spanning subgraphs ($CSSG$) of G ; and (iv) $T(G, 2, 2) = N_{SSG}(G) = 2^{e(G)}$, the number of spanning subgraphs (SSG) of G . For both the open and cyclic strips, the last of these quantities is directly determined by Eq. (2.3) as

$$N_{SSG}(G_{\{e\}_r, e_g, m; BC}) = 2^{e(G_{\{e\}_r, e_g, m; BC})} = 2^{m[(\sum_{j=1}^r e_j) + e_g]} . \quad (13.1)$$

The evaluation of our general results for $T(G_{\{e\}_r, e_g, m; o}, x, y)$ and $T(G_{\{e\}_r, e_g, m; c}, x, y)$ for the requisite values of x and y yield the above-mentioned graphical quantities (i)-(iii). We discuss these next.

B. Spanning Trees

To evaluate the number of spanning trees of the hammock chain graphs, $N_{ST}(G_{\{e\}_r, e_g, m; BC})$, we require the evaluation of $T(G_{\{e\}_r, e_g, m; BC}, 1, 1)$. Using the general formulas given in the text, we calculate

$$N_{ST}(G_{\{e\}_r, e_g, m; o}) = (\lambda_{T, 0; x=1, y=1})^m , \quad (13.2)$$

where

$$\lambda_{T, 0; x=1, y=1} = \sum_{r \text{ terms}} \left(\prod_j e_j \right)_{r-1} , \quad (13.3)$$

and the notation $(\prod_j e_j)_{r-1}$ means the product of the edges in the set $\{e\}_r$ with one edge removed. Since there are r ways of removing one edge from this product, there are r terms in the sum of $(r-1)$ -fold products in Eq. (13.3). For the cyclic chain, we find

$$N_{ST}(G_{\{e\}_r, e_g, m; c}) = m(\lambda_{T, 0; x=1, y=1})^{m-1} \left[e_g \lambda_{T, 0; x=1, y=1} + \prod_{j=1}^r e_j \right] . \quad (13.4)$$

For $r = 2$, these general formulas yield

$$N_{ST}(G_{\{e\}_{r=2}, e_g, m; o}) = (e_1 + e_2)^m \quad (13.5)$$

and

$$N_{ST}(G_{\{e\}_{r=2}, e_g, m; c}) = m(e_1 + e_2)^{m-1} \left[e_g(e_1 + e_2) + e_1 e_2 \right] , \quad (13.6)$$

in agreement with Eqs. (11.2) and (11.3) in [24]. As an example of an explicit result for higher r , for $r = 3$, the general results above yield

$$N_{ST}(G_{\{e\}_{r=3,e_g,m;o}}) = (e_1e_2 + e_1e_3 + e_2e_3)^m \quad (13.7)$$

and

$$N_{ST}(G_{\{e\}_{r=3,e_g,m;c}}) = m(e_1e_2 + e_1e_3 + e_2e_3)^{m-1} \left[e_g(e_1e_2 + e_1e_3 + e_2e_3) + e_1e_2e_3 \right]. \quad (13.8)$$

C. Spanning Forests

Substituting $x = 2$ and $y = 1$ in our general calculation of the Tutte polynomials, we obtain $N_{SF}(G_{\{r\}_{r,e_g,m;o}}$ and $N_{SF}(G_{\{r\}_{r,e_g,m;c}}$ for arbitrary r . These

$$N_{SF}(G_{\{e\}_{r,e_g,m;o}}) = (\lambda_{T,0;x=2,y=1})^m \quad (13.9)$$

and

$$N_{SF}(G_{\{e\}_{r,e_g,m;c}}) = (\lambda_{T,0;x=2,y=1})^m - (\lambda_{T,1;x=2,y=1})^m, \quad (13.10)$$

where these $\lambda_{T,0}$ and $\lambda_{T,1}$ evaluated at $x = 2$ and $y = 1$ (and hence $q = 0$) are

$$\begin{aligned} \lambda_{T,0;x=2,y=1} = & 2^{e_g} \left[2^{(\sum e_j)r} - \theta(r-3) \sum_{\binom{r}{2} \text{ terms}} 2^{(\sum e_j)r-2} \right. \\ & \left. + 2\theta(r-4) \sum_{\binom{r}{3} \text{ terms}} 2^{(\sum e_j)r-3} + \dots + (-1)^{r-1}(r-1) \right] \end{aligned} \quad (13.11)$$

and

$$\begin{aligned} \lambda_{T,1;x=2,y=1} = & \theta(r-2) \sum_{r \text{ terms}} 2^{(\sum e_j)r-1} - 2\theta(r-3) \sum_{\binom{r}{2} \text{ terms}} 2^{(\sum e_j)r-2} \\ & + 3\theta(r-4) \sum_{\binom{r}{3} \text{ terms}} 2^{(\sum e_j)r-3} + \dots + (-1)^{r+1}r. \end{aligned} \quad (13.12)$$

Here we have used the identity $D_n = (-1)^n(n-1)$ at $q = 0$, from Eq. (17.2).

For the special case $r = 2$ these general formulas reduce to

$$N_{SF}(G_{\{e\}_{r=2,e_g,m;o}}) = \left[2^{e_g} \left(2^{e_1+e_2} - 1 \right) \right]^m \quad (13.13)$$

and

$$N_{SF}(G_{\{e\}_{r=2,e_g,m;c}}) = \left[2^{e_g} \left(2^{e_1+e_2} - 1 \right) \right]^m - \left[2^{e_1} + 2^{e_2} - 2 \right]^m, \quad (13.14)$$

in agreement with Eqs. (11.4) and (11.5) in [24].

As an illustration of the application of our general results to a higher- r case, we consider $r = 3$. Here we calculate

$$N_{SF}(G_{\{e\}_{r=3,e_g,m;o}}) = \left[2^{e_g} \left\{ 2^{e_1+e_2+e_3} - (2^{e_1} + 2^{e_2} + 2^{e_3}) + 2 \right\} \right]^m \quad (13.15)$$

and

$$\begin{aligned} N_{SF}(G_{\{e\}_{r=3,e_g,m;c}}) &= \left[2^{e_g} \left\{ 2^{e_1+e_2+e_3} - (2^{e_1} + 2^{e_2} + 2^{e_3}) + 2 \right\} \right]^m \\ &- \left[\left(2^{e_1+e_2} + 2^{e_1+e_3} + 2^{e_2+e_3} \right) - 2 \left(2^{e_1} + 2^{e_2} + 2^{e_3} \right) + 3 \right]^m. \end{aligned} \quad (13.16)$$

The numbers $N_{SF}(G_{\{e\}_{r,e_g,m;o}})$ and $N_{SF}(G_{\{e\}_{r,e_g,m;c}})$ for higher r can be computed in a similar manner from our general expressions for the Tutte polynomials.

D. Connected Spanning Subgraphs

By substituting $x = 1$ and $y = 2$ in our general results, one can calculate N_{CSSG} for these hammock chain graphs. Again, it is useful to utilize Eqs. (3.18) and (3.19) for this purpose. Carrying out this procedure, we obtain, for the open hammock chain graphs,

$$N_{CSSG}(G_{\{e\}_{r,e_g,m;o}}) = (\lambda_{T,0;x=1,y=2})^m, \quad (13.17)$$

where

$$\lambda_{T,0;x=1,y=2} = \prod_{j=1}^r (e_j + 1) - \prod_{j=1}^r e_j \quad (13.18)$$

For the cyclic hammock chain graphs we calculate

$$N_{CSSG}(G_{\{e\}_{r,e_g,m;c}}) = (\lambda_{T,0;x=1,y=2})^{m-1} \left[(me_g + 1) \lambda_{T,0;x=1,y=2} + m \prod_{j=1}^r e_j \right]. \quad (13.19)$$

For $r = 2$, these general results yield

$$N_{CSSG}(G_{\{e\}_{r=2,e_g,m;o}}) = (e_1 + e_2 + 1)^m \quad (13.20)$$

and

$$N_{CSSG}(G_{\{e\}_{r=2,e_g,m;c}}) = (e_1 + e_2 + 1)^{m-1} \left[(me_g + 1)(e_1 + e_2 + 1) + me_1e_2 \right], \quad (13.21)$$

in agreement with Eqs. (11.6) and (11.7) of [24]. As an example of a result for higher r , in the case $r = 3$, the general results above yield

$$N_{CSSG}(G_{\{e\}_{r=3,e_g,m;o}}) = (\lambda_{T,0;x=1,y=2,r=3})^m \quad (13.22)$$

and

$$N_{CSSG}(G_{\{e\}_{r=3,e_g,m;c}}) = (\lambda_{T,0;x=1,y=2,r=3})^{m-1} \times \left[(me_g + 1)\lambda_{T,0;x=1,y=2,r=3} + me_1e_2e_3 \right], \quad (13.23)$$

where

$$\lambda_{T,0;x=1,y=2,r=3} = (e_1e_2 + e_1e_3 + e_2e_3) + (e_1 + e_2 + e_3) + 1. \quad (13.24)$$

E. Acyclic and Cyclic Orientations

Assigning an orientation to each edge $e \in E$ of a graph $G = (V, E)$ yields a directed graph, denoted $G = (V, \vec{E})$. Among the $2^{e(G)}$ edge orientations, an acyclic orientation of G is defined as an orientation that does not contain any directed cycles. A directed cycle is a cycle in which, as one travels along the cycle, all of the oriented edges have the same direction. The number of such acyclic orientations is denoted $a(G)$. This quantity depends only on the structure of the basic graph G itself and given by the evaluation of the Tutte polynomial of G with $x = 2$ and $y = 0$ [60]:

$$a(G) = T(G, 2, 0). \quad (13.25)$$

Equivalently, this is obtained by the evaluation of the chromatic polynomial at $q = -1$: $a(G) = (-1)^{n(G)} P(G, -1)$. For the oriented graph $G = (V, \vec{E})$, a totally cyclic orientation is one in which every oriented edge is a member of a directed cycle. The number of totally cyclic edge orientations, denoted $b(G)$, again depends only on the structure of the basic graph G is given by [61]

$$b(G) = T(G, 0, 2). \quad (13.26)$$

From our general calculation of the Tutte polynomials for the open and cyclic hammock chain graphs, we have, for general r ,

$$a(G_{\{e\}_{r,e_g,m;o}}) = (\lambda_{T,0;x=2,y=0})^m \quad (13.27)$$

and

$$a(G_{\{e\}_{r,e_g,m;c}}) = (\lambda_{T,0;x=2,y=0})^m - 2(\lambda_{T,1;x=2,y=0})^m, \quad (13.28)$$

where

$$\lambda_{T,0;x=2,y=0} = 2^{e_g} \left[2 \prod_{j=1}^r (2^{e_j} - 1) - \prod_{j=1}^r (2^{e_j} - 2) \right] \quad (13.29)$$

and

$$\lambda_{T,1;x=2,y=0} = \prod_{j=1}^r (2^{e_j} - 1) - \prod_{j=1}^r (2^{e_j} - 2). \quad (13.30)$$

For $r = 2$, these general formulas reduce to

$$a(G_{\{e\}_{r=2,e_g,m;o}}) = \left[2^{e_g} \left(2^{e_1+e_2} - 2 \right) \right]^m \quad (13.31)$$

and

$$a(G_{\{e\}_{r=2,e_g,m;c}}) = \left[2^{e_g} \left(2^{e_1+e_2} - 2 \right) \right]^m - 2 \left[2^{e_1} + 2^{e_2} - 3 \right]^m, \quad (13.32)$$

in agreement with Eqs. (11.9) and (11.10) in [24]. As an explicit example of cases with higher r , for $r = 3$, we have

$$a(G_{\{e\}_{r=3,e_g,m;o}}) = (\lambda_{T,0;x=2,y=0,r=3})^m \quad (13.33)$$

and

$$a(G_{\{e\}_{r=3,e_g,m;c}}) = (\lambda_{T,0;x=2,y=0,r=3})^m - 2(\lambda_{T,0;x=2,y=0,r=3})^m, \quad (13.34)$$

where

$$\lambda_{T,0;r=3,x=2,y=0} = 2^{e_g} \left[2^{e_1+e_2+e_3} - 2 \left(2^{e_1} + 2^{e_2} + 2^{e_3} \right) + 6 \right] \quad (13.35)$$

and

$$\lambda_{T,1;r=3,x=2,y=0} = \left(2^{e_1+e_2} + 2^{e_1+e_3} + 2^{e_2+e_3} \right) - 3 \left(2^{e_1} + 2^{e_2} + 2^{e_3} \right) + 7. \quad (13.36)$$

From our general results for Tutte polynomials of hammock chain graphs, we find, for the number of totally cyclic orientations on these graphs,

$$b(G_{\{e\}_{r,e_g,m;o}}) = \delta_{e_g,0} (2^r - 2)^m \quad (13.37)$$

and

$$b(G_{\{e\}_{r,e_g,m;c}}) = 2(2^r - 1)^m - \delta_{e_g,0} (2^r - 2)^m. \quad (13.38)$$

XIV. CONCLUSIONS

In conclusion, in this paper we have presented exact calculations of the Potts/Tutte polynomials for hammock chain graphs $G_{\{e_1, \dots, e_r\}, e_g, m; BC}$ comprised of m repeated hammock (series-parallel) subgraphs H_{e_1, \dots, e_r} connected with line graphs of length e_g edges, such that the chains have open or cyclic boundary conditions (BC). We study the general case where the hammock subgraphs H_{e_1, \dots, e_r} have r separate paths along “ropes” with respective lengths e_1, \dots, e_r edges connecting the two end-vertices of each hammock subgraph. We have discussed the special cases of these results that yield chromatic polynomials, flow polynomials, reliability polynomials, and various quantities of graph-theoretic interest, including numbers of spanning trees, spanning forests, connected spanning subgraphs, acyclic orientations, and cyclic orientations. We have presented a detailed study of the continuous accumulation set \mathcal{B}_q of chromatic zeros in the complex q plane in the limit of infinite chain length, $m \rightarrow \infty$, for a variety of choices of edge sets $(\{e\}_r, e_g)$. This work involves a very interesting confluence of statistical mechanics, graph theory, complex analysis, and algebraic geometry.

XV. ACKNOWLEDGMENTS

This research was partially supported by the U.S. National Science Foundation grant NSF-PHY-22-10533. RS expresses his gratitude to Shan-Ho Tsai for the valuable collaboration on the earlier related work in Refs. [19, 23].

XVI. ETHICS STATEMENTS ON CONFLICT OF INTEREST AND DATA ACCESSIBILITY

As required by current rules for article submission, the authors include the following ethics statements:

1. Concerning any possible conflicts of interest, the authors have no financial or non-financial conflict of interest or competing interests that are relevant to this article. The authors have stated their grant support in the Acknowledgments.
2. Concerning data accessibility, this article is theoretical and does not contain any experimental data. Computational data supporting the conclusions of the article are included herein.

XVII. APPENDIX

For reference we list some special values of D_n here [22].

$$D_n = (-1)^n (2^{n-1} - 1) \quad \text{if } q = -1 \quad (17.1)$$

$$D_n = (-1)^n (n - 1) \quad \text{if } q = 0 \quad (17.2)$$

$$D_n = (-1)^n \quad \text{if } q = 1 \quad (17.3)$$

and

$$D_n = \begin{cases} 1 & \text{if } q = 2 \text{ and } n \text{ is even} \\ 0 & \text{if } q = 2 \text{ and } n \text{ is odd} \end{cases} . \quad (17.4)$$

A factorization property is that if n is odd, say $n = 2k + 1$, then

$$D_{2k+1} \text{ contains the factor } q - 2. \quad (17.5)$$

One can characterize the Taylor expansion of D_{2k+1} further. In addition to $D_3 = q - 2$, the Taylor series of D_{2k+1} about $q = 2$ is

$$D_{2k+1} = k(q - 2) + k(k - 1)(q - 2)^2 + \dots \quad \text{as } q \rightarrow 2, \quad (17.6)$$

where the $+\dots$ indicate higher-order terms in the Taylor expansion of D_{2k+1} about $q = 2$ that are present if $k \geq 2$. D_n satisfies a number of other identities such as

$$D_n = (q - 1)D_{n-1} + (-1)^n . \quad (17.7)$$

These identities can be proved from the definition of D_n in Eq. (2.30).

References

-
- [1] Potts, R. B.: Some generalized order-disorder transformations. Proc. Cambridge Phil. Soc. **48**, 106-109 (1952)
 - [2] Wu, F. Y.: The Potts model. Rev. Mod. Phys. **54**, 235-268 (1982)
 - [3] Birkhoff, G. D.: On the number of ways of coloring a map. Proc. Edinburgh Math. Soc. **2**, 83-91 (1930).

- [4] Whitney, H.: The coloring of graphs. *Ann. Math.* **33**, 688-718 (1932)
- [5] Read, R. C. and Tutte, W. T.: Chromatic polynomials, in *Selected Topics in Graph Theory 3*, eds. Beineke, L. W. and Wilson, R. J. (Academic Press, New York, 1988) 15-42
- [6] Read, R. C. and Royle, G. F.: Chromatic roots of families of graphs, in *Graph Theory, Combinatorics, and Applications* eds. Alavi Y, Chartrand G, Ollermann O R, and Schwenk A J (Wiley, New York, 1991)
- [7] Dong, F. M., Koh, K. M., and Teo, K. L.: *Chromatic Polynomials and Chromaticity of Graphs* (World Scientific, Singapore, 2005)
- [8] Baxter, R. J.: Colourings of a hexagonal lattice. *J. Math. Phys.* **11**, 784-789 (1970)
- [9] Baxter, R. J.: q -Colourings of the triangular lattice. *J. Phys. A* **19**, 2821-2839 (1986)
- [10] Baxter, R. J.: Chromatic polynomials of large triangular lattices. *J. Phys. A* **20**, 5241-5261 (1987)
- [11] Pauling, L.: The structure and entropy of ice and other crystals with some randomness of atomic arrangement. *J. Am. Chem. Soc.* **57**, 2680-2684 (1935)
- [12] Nagle, J. F.: Lattice statistics of hydrogen-bonded crystals. I the residual entropy of ice. *J. Math. Phys.* **7**, 1484-1491 (1966)
- [13] Lieb, E. H.: 1967 Residual entropy of square ice. *Phys. Rev.* **162**, 162-172 (1967)
- [14] Tutte, W. T.: A ring in graph theory. *Proc. Cambridge Phil. Soc.* **43**, 26-40 (1947)
- [15] Tutte, W. T.: A contribution to the theory of chromatic polynomials. *Canad. J. Math.* **6**, 80-91 (1954)
- [16] Tutte, W. T.: On dichromatic polynomials. *J. Combin. Theory* **2** 301-320 (1967)
- [17] Bollobás, B.: *Modern Graph Theory* (Springer, New York, 1998)
- [18] Welsh, D. J. A.: *Complexity: Knots, Colouring, and Counting* (Cambridge University Press, Cambridge, UK, 1993)
- [19] Shrock, R. and Tsai, S.-H.: Ground state degeneracy of Potts antiferromagnets: Cases with noncompact W boundaries having multiple points at $1/q = 0$. *J. Phys. A* **31** 9641-9665 (1998)
- [20] Shrock, R. and Tsai, S.-H.: Asymptotic limits and zeros of chromatic polynomials and ground state entropy of Potts antiferromagnets. *Phys. Rev. E* **55**, 5165-5179 (1997)

- [21] Shrock, R. and Tsai, S.-H.: Families of graphs with $W_r(\{G\}, q)$ functions that are nonanalytic at $1/q = 0$. Phys. Rev. E **56**, 3935-3943 (1997)
- [22] Shrock, R. and Tsai, S.-H.: Ground state degeneracy of Potts antiferromagnets: Homeomorphic classes with noncompact W boundaries. Physica A **265**, 186-223 (1999)
- [23] Shrock, R. and Tsai, S.-H.: Ground state entropy of Potts antiferromagnets on cyclic polygon chain graphs. J. Phys. A **32**, 5053-5070 (1999)
- [24] Shrock, R.: Exact Potts/Tutte polynomials for polygon chain graphs. J. Phys. A **44**, 145002 (2011)
- [25] Biggs, N. L., Damerell, R. M., and Sands, D. A.: Recursive families of graphs. J. Combin. Theory B **12**, 123-131 (1972)
- [26] Biggs, N.: *Algebraic Graph Theory* (Cambridge University Press, Cambridge, UK, 1993)
- [27] Sokal, A. D.: Chromatic roots are dense in the whole complex plane. Combin. Probab. Comput. **13**, 221-261 (2004)
- [28] Brown, J. I., Hickman, C. A., Sokal, A. D., and Wagner, D. G.: On the chromatic roots of generalized Theta graphs. J. Combin. Theory B **83**, 272-297 (2001)
- [29] Fortuin, C. M. and Kasteleyn, P. W.: On the random cluster model. Physica **57**, 536-564 (1972)
- [30] Shrock, R. and Tsai, S.-H.: Ground state entropy of Potts antiferromagnets on homeomorphic families of strip graphs. Physica A **259**, 315-348 (1998)
- [31] Shrock, R.: Exact Potts model partition functions for ladder graphs. Physica A **283**, 388-446 (2000)
- [32] Woodall, D. R.: Zeros of chromatic polynomials, in Proc. of the Sixth British Combinatorial Conference, ed. P. J. Cameron (Academic Press, New York, 1977), pp. 199-223
- [33] Jackson, B.: A zero-free interval for chromatic polynomials of graphs. Combin. Probab. Comput. **2**, 325-336 (1993)
- [34] Thomassen, C.: The zero-free intervals for chromatic polynomials of graphs. Combin. Probab. Comput. **6**, 497-506 (1997)
- [35] Beraha, S., Kahane, J., and Weiss, N.: Limits of zeros of recursively defined families of poly-

- nomials, in *Studies in Foundations and Combinatorics, Advances in Mathematics and Supplementary Studies, vol. 1*, Rota G C ed. (Academic Press, New York, 1978) 213-232
- [36] Beraha, S., Kahane, J., and Weiss, N.: Limits of chromatic zeros of some families of maps. *J. Combin. Theory B* **28**, 52-65 (1980)
- [37] Hartshorne, R.: *Algebraic Geometry* (Springer, New York, 1977)
- [38] Shafarevich, I. R.: *Basic Algebraic Geometry* (Springer, New York, 1977)
- [39] Wilson, G.: Hilbert's sixteenth problem. *Topology* **17**, 53-73 (1978)
- [40] Roček, M., Shrock, R., and Tsai, S.-H.: Chromatic polynomials for families of strip graphs and their asymptotic limits. *Physica A* **252**, 505-546 (1998)
- [41] Shrock, R. and Tsai, S.-H.: Ground state entropy of the Potts antiferromagnet on cyclic strip graphs. *J. Phys. A Letts.* **32**, L195-L200 (1999)
- [42] Shrock, R. and Tsai, S.-H.: Ground state degeneracy of Potts antiferromagnets on 2D lattices: approach using infinite cyclic strip graphs. *Phys. Rev. E* **60**, 3512-3515 (1999)
- [43] Chang, S.-C. and Shrock, R.: Ground state entropy of the Potts antiferromagnet on strips of the square lattice. *Physica A* **290**, 402-430 (2001)
- [44] Chang, S.-C. and Shrock, R.: Exact Potts model partition functions on strips of the honeycomb lattice. *Physica A* **296**, 183-233 (2001)
- [45] Chang S.-C. and Shrock R.: Exact Potts model partition functions on wider arbitrary-length strips of the square lattice. *Physica A* **296**, 234-288 (2001)
- [46] Salas, J. and Sokal, A. D.: Transfer matrices and partition-function zeros for antiferromagnetic Potts models. I. General theory and square-lattice chromatic polynomial. *J. Stat. Phys.* **104** 609-699 (2001)
- [47] Jacobsen, J. L. and Salas, J.: Transfer matrices and partition-function zeros for antiferromagnetic Potts models. II. Extended results for square-lattice chromatic polynomial. *J. Stat. Phys.* **104**, 701-723 (2001)
- [48] Salas, J. and Shrock, R.: Exact $T = 0$ partition functions for Potts antiferromagnets on sections of the simple cubic lattice. *Phys. Rev. E* **64**, 011111 (2001)
- [49] Chang, S.-C. and Shrock, R.: General structural results for Potts model partition functions

- on lattice strips. *Physica A* **316**, 335-379 (2002)
- [50] Chang, S.-C., Salas, J., and Shrock, R.: Exact Potts model partition functions for strips of the square lattice. *J. Stat. Phys.* **107**, 1207-125 (2002)3
- [51] Chang, S.-C., Jacobsen, J. L., Salas, J., and Shrock, R.: Exact Potts model partition functions for strips of the triangular lattice, *J. Stat. Phys.* **114** 763-822 (2004)
- [52] Beaudin, L., Ellis-Monaghan, J., Pangborn, G., and Shrock, R.: A little statistical mechanics for the graph theorist. *Discr. Math.* **310**, 2037-2053 (2010)
- [53] Ford, L. and Fulkerson, D.: *Flows in Networks* (Princeton University Press, Princeton, 1962)
- [54] Chang, S.-C. and Shrock, R.: Flow polynomials and their asymptotic limits for lattice strip graphs. *J. Stat. Phys.* **112**, 815-879 (2003)
- [55] Colbourn, C.: *The Combinatorics of Network Reliability* (Oxford University Press, New York, 1987)
- [56] Brown, J. I., Colbourn, C. J., Cox, D., Graves, C., and Mol, L.: Network reliability: heading out on the highway. *Networks* **77**, 146-160 (2020)
- [57] Chang, S.-C. and Shrock, R.: Reliability polynomials and their asymptotic limits for lattice strips. *J. Stat. Physics* **112**, 1019-1077 (2003)
- [58] Stauffer, D. and Aharony, A.: *Introduction to Percolation Theory* (Taylor and Francis, London, 1991)
- [59] Bollobás, B. and Riordan, O.: *Percolation* (Cambridge University Press, Cambridge, UK, 2006)
- [60] Stanley, R. P.: Acyclic orientations of graphs. *Discrete Math.* **5**, 171-178 (1973)
- [61] Las Vergnas, M.: Acyclic and totally cyclic orientations of combinatorial geometries. *Discrete Math.* **20**, 51-61 (1977)
- [62] Chang, S.-C. and Shrock, R.: Asymptotic behavior of acyclic and cyclic orientations of directed lattice graphs. *Physica A* **540**, 123059 (2020)